EFT analyses for the top quark sector

Alexander Grohsjean

HELMHOLTZ
RESEARCH FOR GRAND CHALLENGES

ZPW 2020 - The Higgs boson and the top quark

13^{th} - 15^{th} January 2020

University of Zürich

25 years ago …

… a few weeks later …

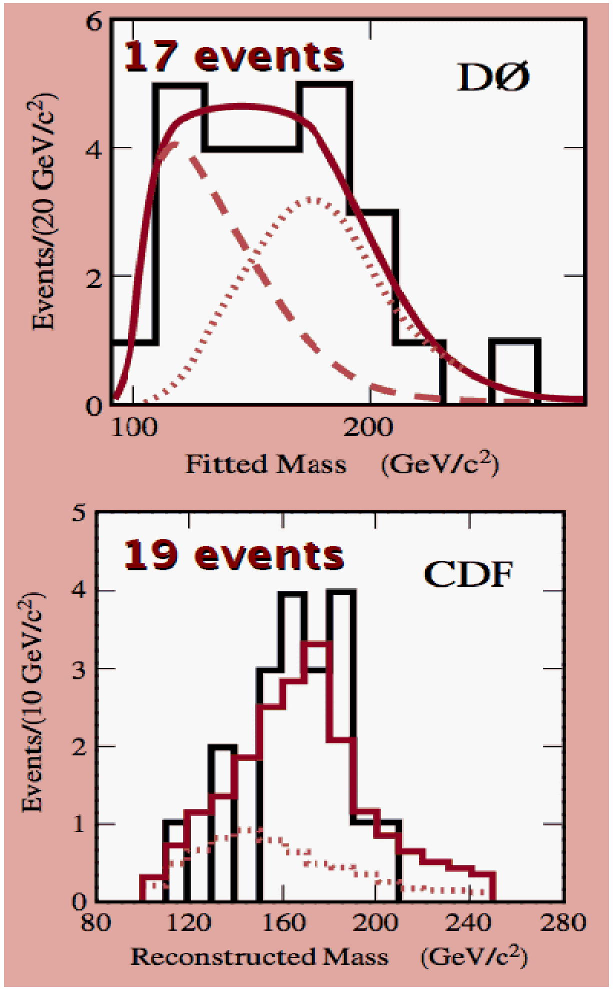

… today

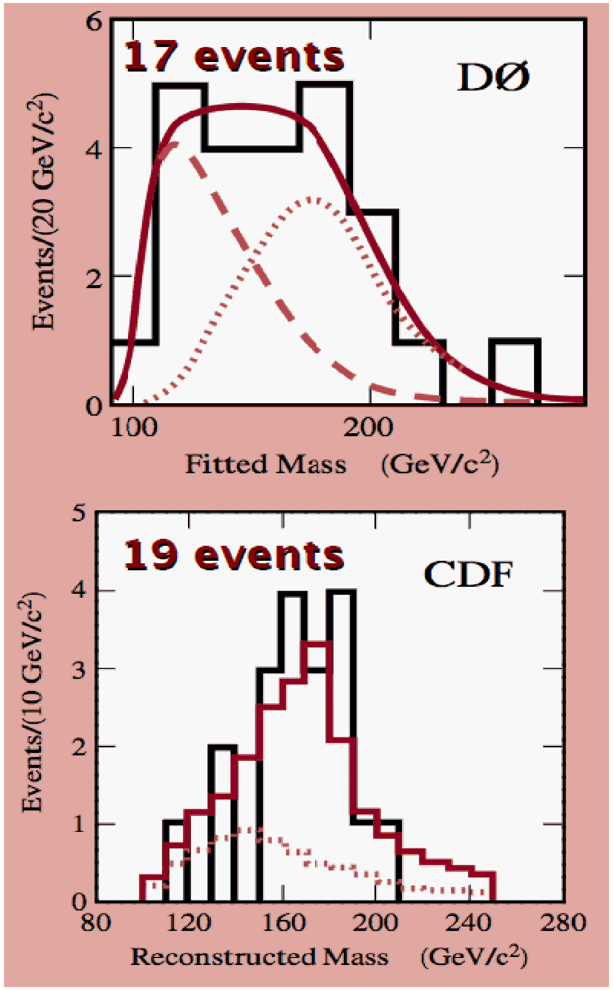

ATLAS-CONF-2019-044

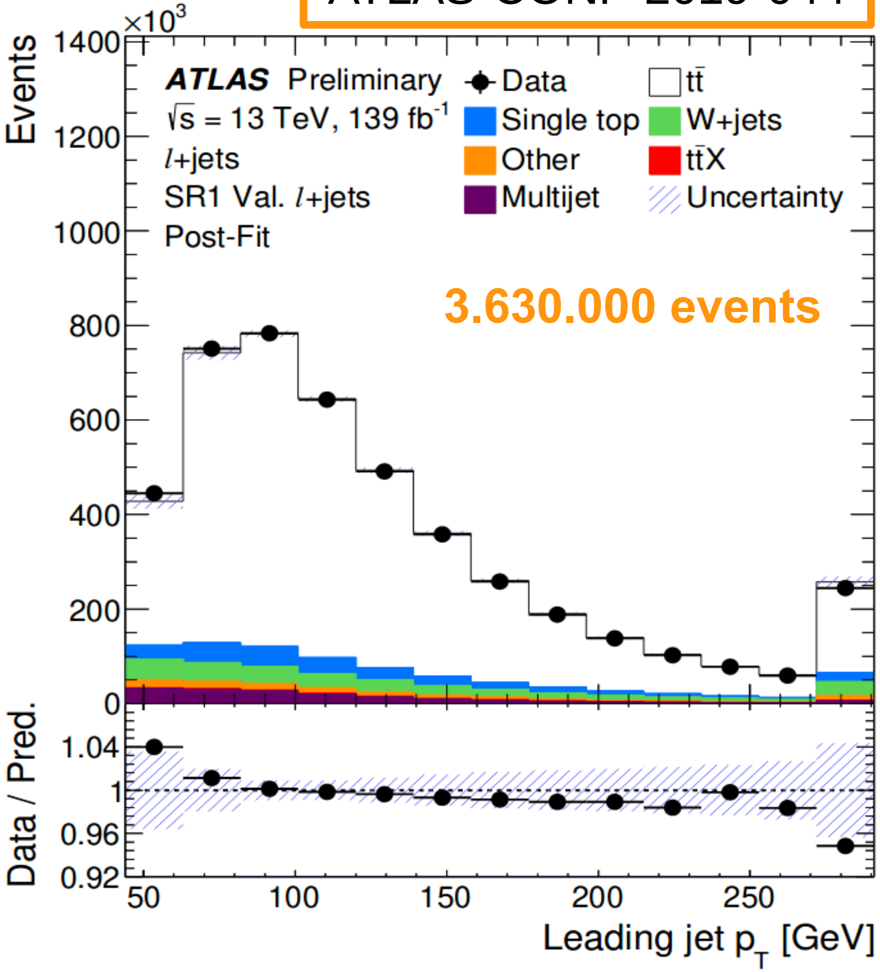

… today

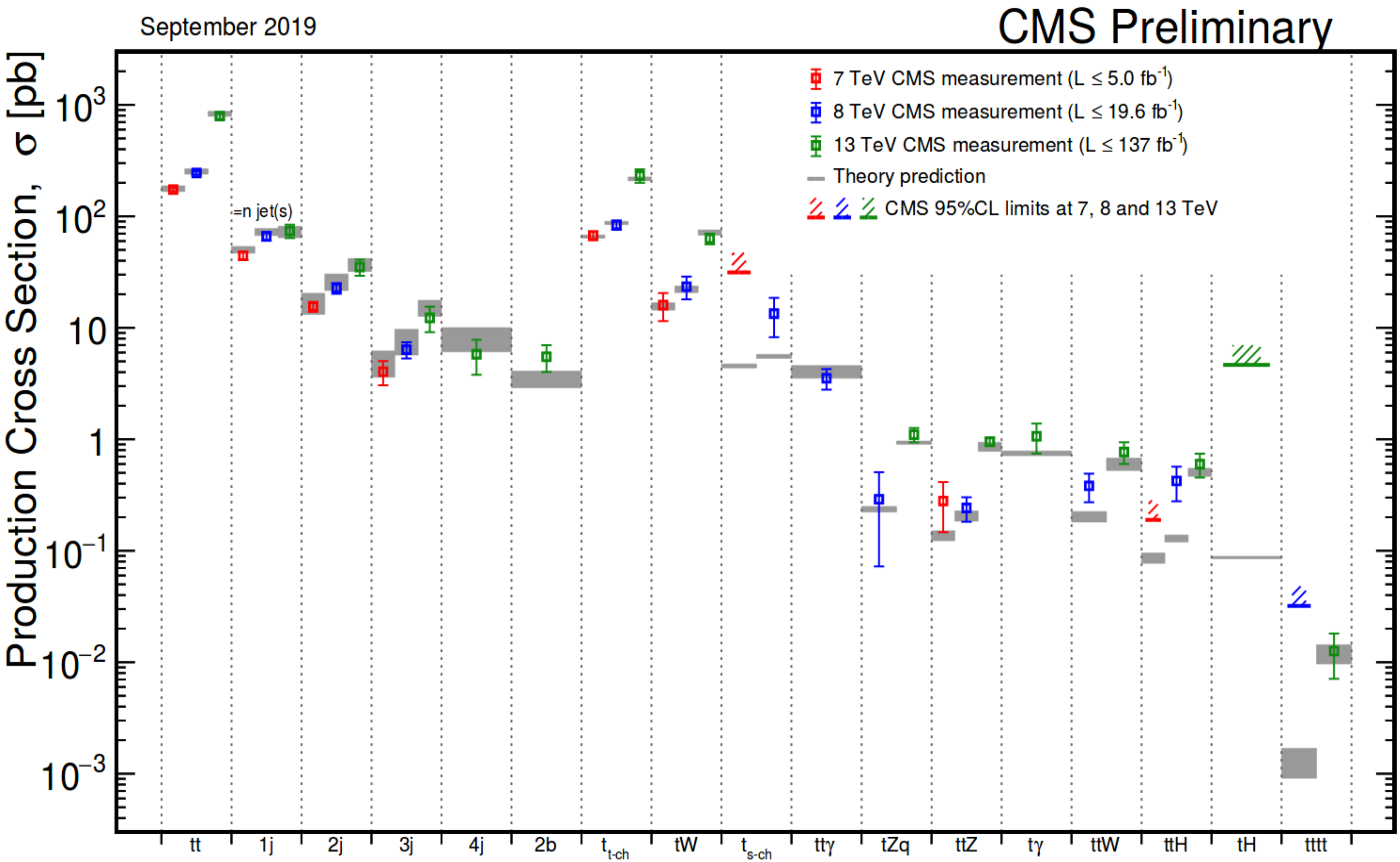

probing about 6 orders of magnitude in top production cross section

… today

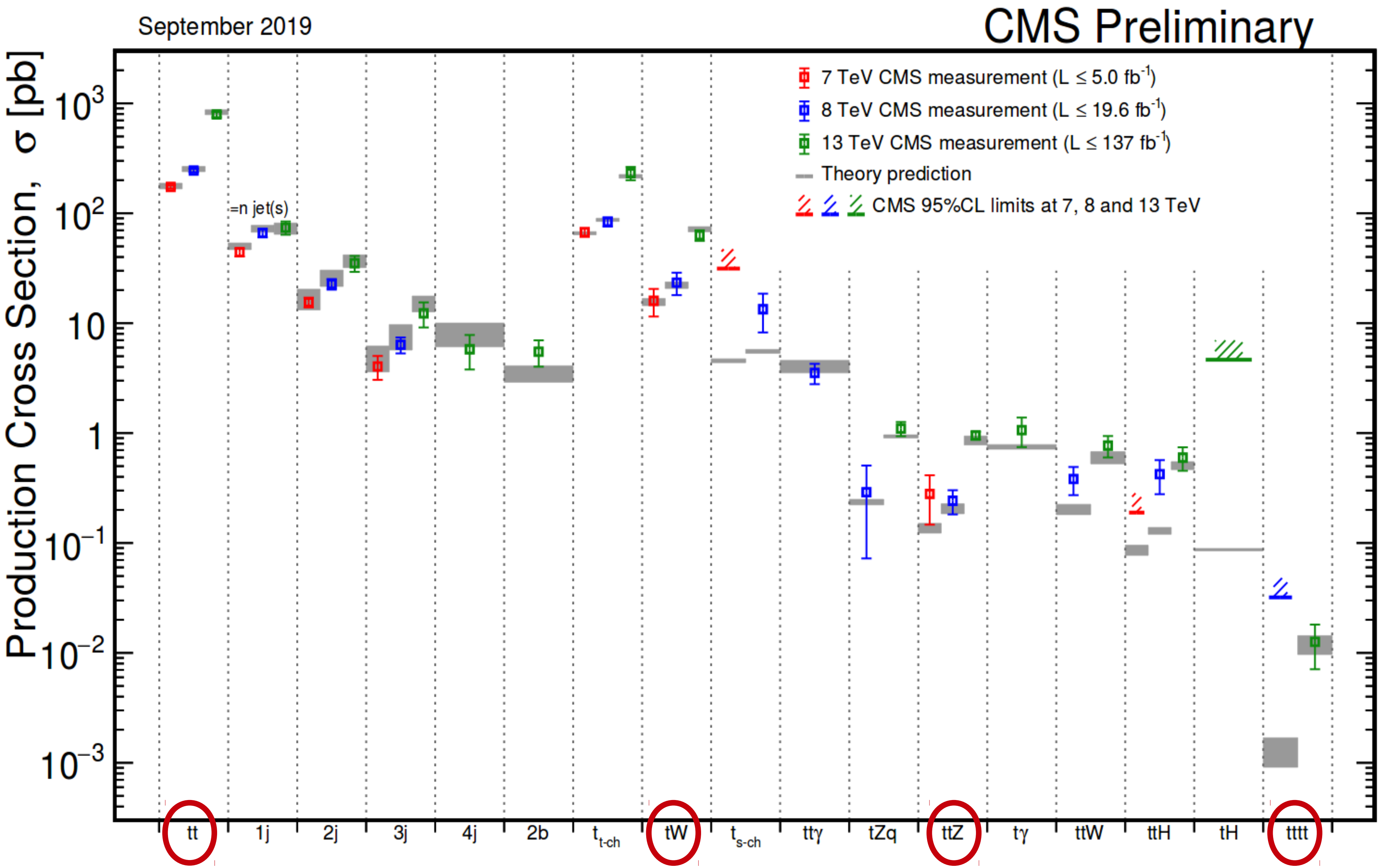

need a common language for (BSM) interpretation : effective field theory

EFT Approaches in ATLAS and CMS

inclusive cross sections

- simple EFT parameterization sufficient

re-interpretation of unfolded measurement → direct measurement from detector-level data

EFT Approaches in ATLAS and CMS

inclusive cross sections

- simple EFT parameterization sufficient

re-interpretation of unfolded measurement → direct measurement from detector-level data

unfolded, differential cross sections

- parton or particle level
- needs differential MC EFT information

EFT Approaches in ATLAS and CMS

inclusive cross sections

- simple EFT parameterization sufficient

hybrid measurement at detector-level

- (SM+EFT)/SM reweighting at generator-level, direct comparison to data
- take SM shape, estimate SM+EFT yields from simulation at generator

re-interpretation of unfolded measurement → direct measurement from detector-level data

unfolded, differential cross sections

- parton or particle level
- needs differential MC EFT information

EFT Approaches in ATLAS and CMS

hybrid measurement at detector-level

- (SM+EFT)/SM reweighting at generator-level, direct comparison to data
- take SM shape, estimate SM+EFT yields from simulation at generator

inclusive cross sections

- simple EFT parameterization sufficient

re-interpretation of unfolded measurement → direct measurement from detector-level data

unfolded, differential cross sections

- parton or particle level
- needs differential MC EFT information

direct measurement of EFT

- no SM assumption
- consider EFT in all relevant processes
- perform simultaneous fit to multiple regions

EFT Approaches in ATLAS and CMS

- good scalability
- easy combinable beyond LHC
- treat background SM-like
- full phase space results sensitive to efficiency/acceptance differences → fiducial

re-interpretation of unfolded measurement → direct measurement from detector-level data

- excellent sensitivity
- probe EFT in all contributing processes
- several options for later combinations, little experience so far in top community

hybrid measurement at detector-level

- (SM+EFT)/SM reweighting at generator-level, direct comparison to data
- take SM shape, estimate SM+EFT yields from simulation at generator

inclusive cross sections

- simple EFT parameterization sufficient

re-interpretation of unfolded measurement → direct measurement from detector-level data

unfolded, differential cross sections

- parton or particle level
- needs differential MC EFT information

direct measurement of EFT

- no SM assumption
- consider EFT in all relevant processes
- perform simultaneous fit to multiple regions

Probing four-fermion operators in $t\bar{t}t\bar{t}$ production

- not yet observed (σ_{SM} ~ 9fb @ NLO)
  - O(10^5) smaller than $t\bar{t}$

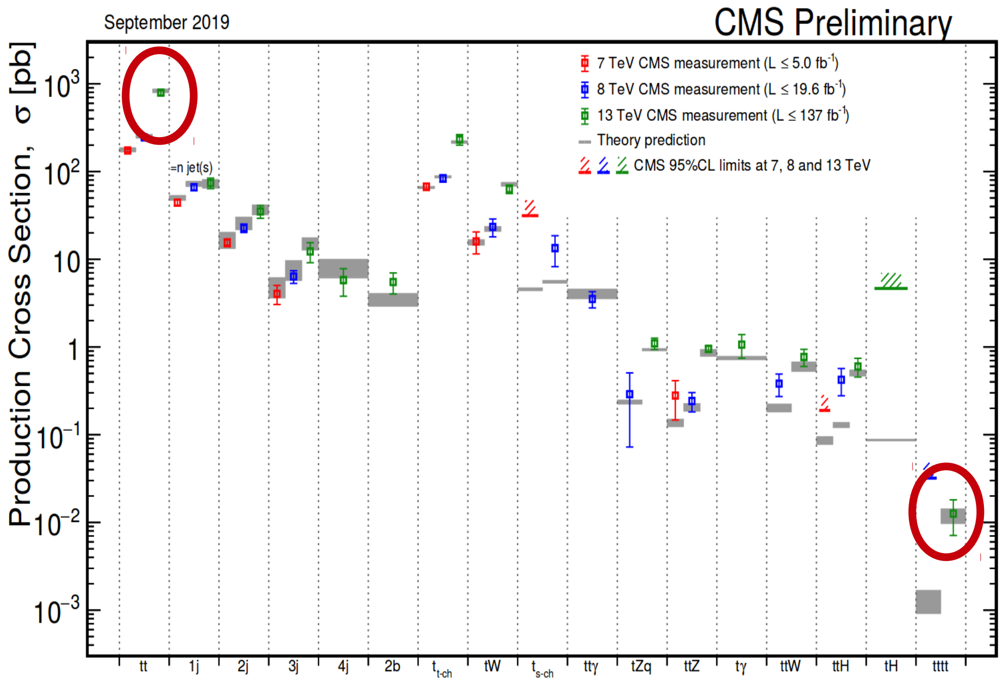

Probing four-fermion operators in $t\bar{t}t\bar{t}$ production

- not yet observed (σ_{SM} ~ 9fb @ NLO)
  - O(10^5) smaller than $t\bar{t}$
- high sensitivity to four heavy-quark operators
  - quadratic cross section contributions up to ~6 fb for coefficient strengths of 1

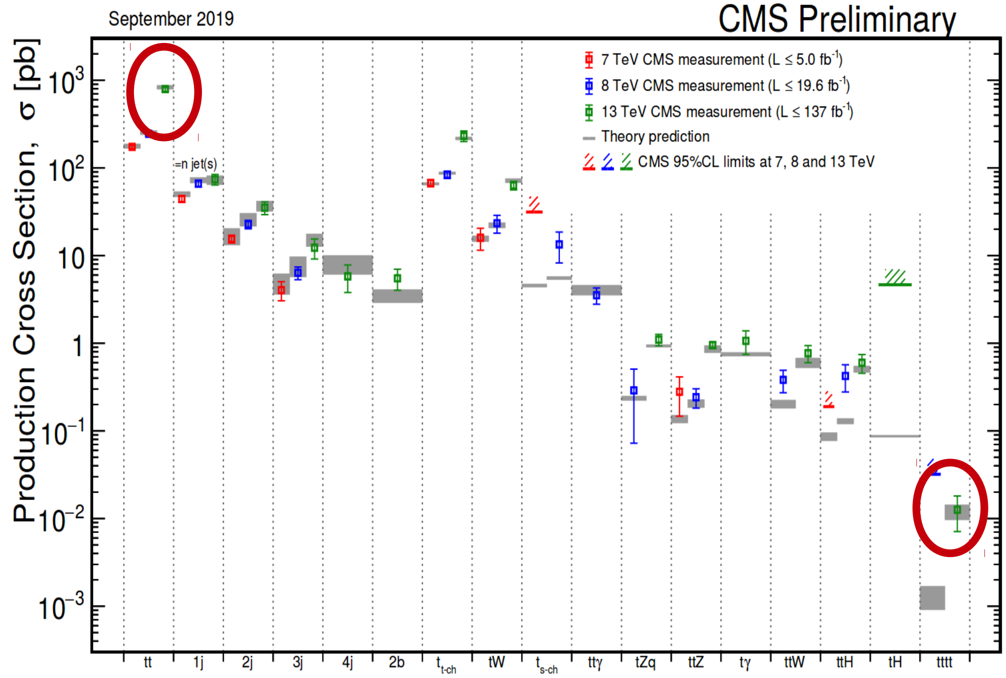

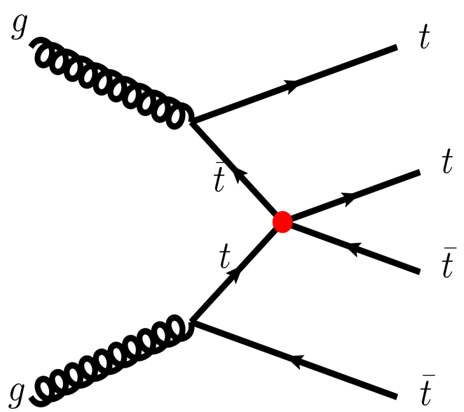

Operator	$\sigma_k^{(1)}$	$\mathcal{O}^1_{tt}$	$\mathcal{O}^1_{QQ}$	$\sigma^{(2)}_{j,k}$ $\mathcal{O}^1_{Qt}$	$\mathcal{O}^8_{Qt}$
$\mathcal{O}^1_{tt}$	0.39	5.59	0.36	−0.39	0.3
$\mathcal{O}^1_{QQ}$	0.47		5.49	−0.45	0.13
$\mathcal{O}^1_{Qt}$	0.03			1.9	−0.08
$\mathcal{O}^8_{Qt}$	0.28				0.45

$$\mathcal{O}^1_{tt} = (\bar{t}_R\gamma^\mu t_R)(\bar{t}_R\gamma_\mu t_R)$$

$$\mathcal{O}^1_{QQ} = (\bar{Q}_L\gamma^\mu Q_L)(\bar{Q}_L\gamma_\mu Q_L)$$

$$\mathcal{O}^1_{Qt} = (\bar{Q}_L\gamma^\mu Q_L)(\bar{t}_R\gamma_\mu t_R)$$

$$\mathcal{O}^8_{Qt} = \left(\bar{Q}_L\gamma^\mu T^A Q_L\right)\left(\bar{t}_R\gamma_\mu T^A t_R\right)$$

$t\bar{t}t\bar{t}$ analysis strategy

- single lepton and opposite-sign dilepton final states
- two dedicated boosted decision trees:
  - identify 3 jet combinations from all-hadronic top decays rather than ISR/FSR (dijet/trijet masses, b-tagging, jet angles, …)

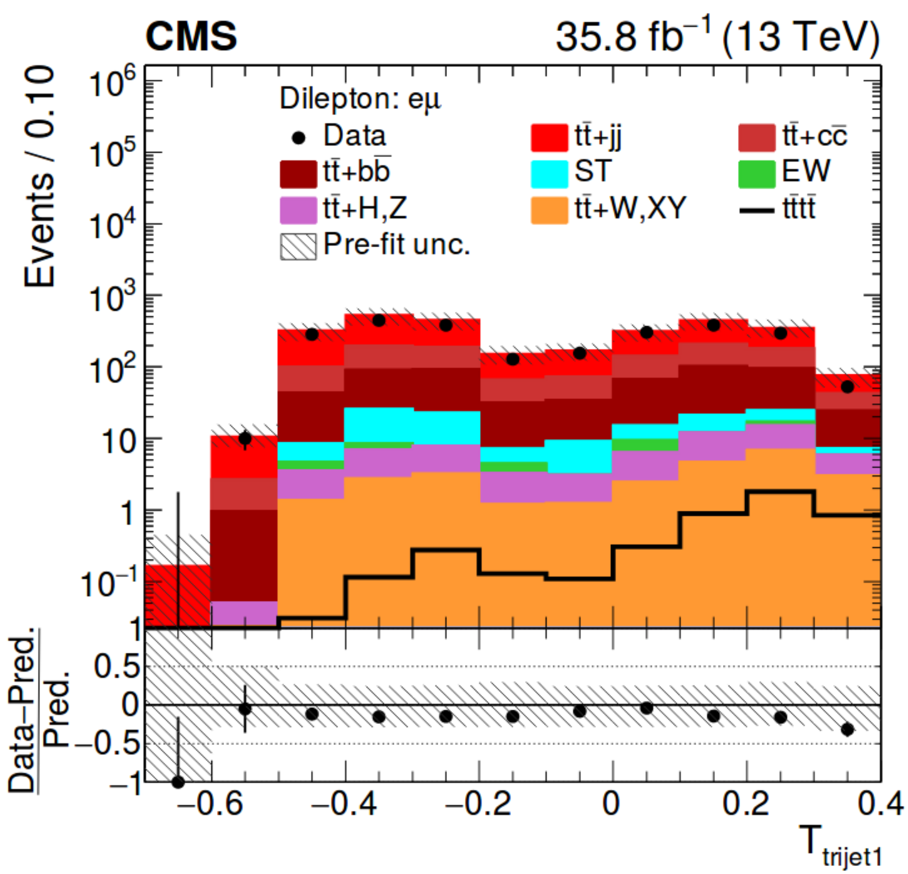

$t\bar{t}t\bar{t}$ analysis strategy

- single lepton and opposite-sign dilepton final states
- two dedicated boosted decision trees:
  - identify 3 jet combinations from all-hadronic top decays rather than ISR/FSR (dijet/trijet masses, b-tagging, jet angles, …)
  - separate $t\bar{t}t\bar{t}$ from $t\bar{t}$ background with different BDTs per final state and jet category

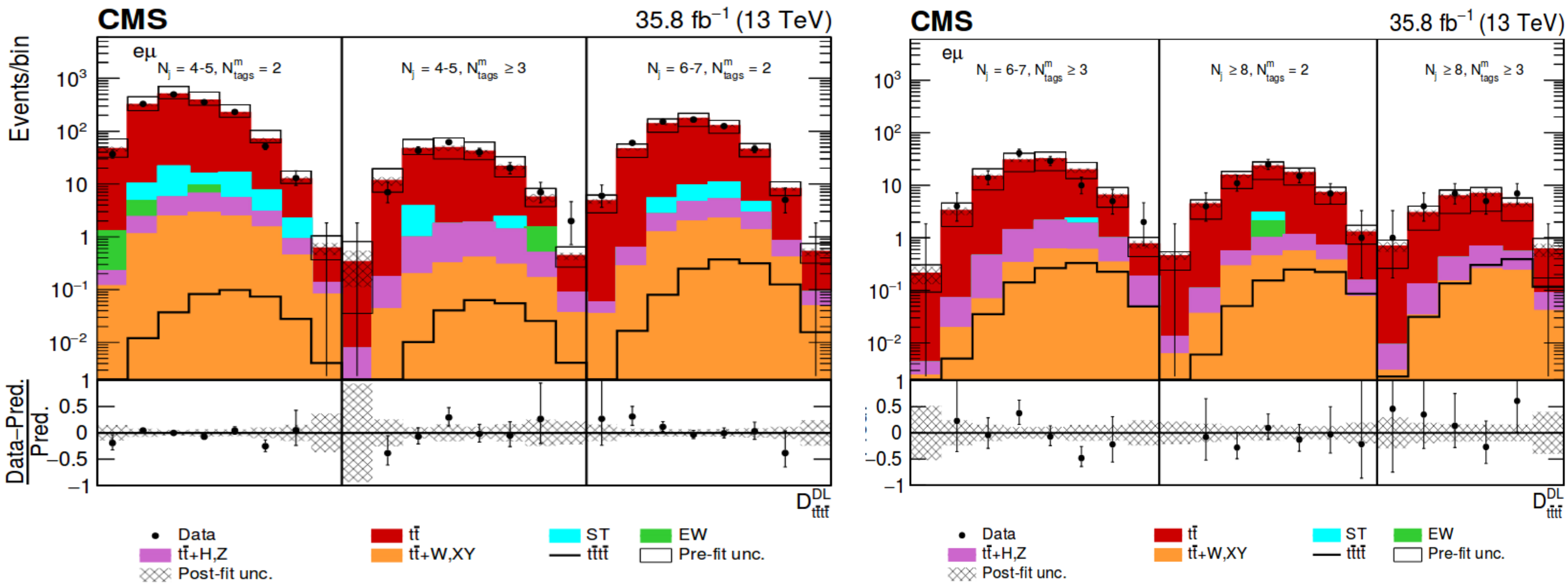

$t\bar{t}t\bar{t}$ cross section results

- combine with same sign dilepton and multilepton analysis (EPJC 78 (2017) 140)

Channel	Expected limit, μ	Observed limit, μ	Expected limit (fb)	Observed limit (fb)
Single-lepton	$9.4^{+4.4}_{-2.9}$	10.6	86^{+40}_{-26}	97
OS dilepton	$7.3^{+4.5}_{-2.5}$	6.9	67^{+41}_{-23}	64
Combined (this analysis)	$5.7^{+2.9}_{-1.8}$	5.2	52^{+26}_{-17}	48
SS dilepton + multilepton	$2.5^{+1.4}_{-0.8}$	4.6	21^{+11}_{-7}	42
Combined (this analysis + [21])	$2.2^{+1.1}_{-0.7}$	3.6	20^{+10}_{-6}	33

1.4 S.D. significance

JHEP 11 (2019) 082

EFT limits from $t\bar{t}t\bar{t}$ production

- at most one additional EFT vertex inserted
- use $t\bar{t}tt$ cross section to constraint heavy-fermion operators
  - assume same kinematics for SM and EFT
- 95% C.L. intervals derived marginalizing contribution of other operators

Operator	Expected C_k/Λ^2 (TeV^{-2})	Observed (TeV^{-2})	Chin. Phys. C42 (2018) 023104
$\mathcal{O}^1_{tt}$	$[-2.0, 1.9]$	$[-2.2, 2.1]$	[-2.92,2.80]
$\mathcal{O}^1_{QQ}$	$[-2.0, 1.9]$	$[-2.2, 2.0]$	
$\mathcal{O}^1_{Qt}$	$[-3.4, 3.3]$	$[-3.7, 3.5]$	[-4.97,4.90]
$\mathcal{O}^8_{Qt}$	$[-7.4, 6.3]$	$[-8.0, 6.8]$	[-10.3,9.33]

JHEP 11 (2019) 082

increased sensitivity compared to previous results

EFT Approaches in ATLAS and CMS

hybrid measurement at detector-level
- (SM+EFT)/SM reweighting at generator-level, direct comparison to data
- take SM shape, estimate SM+EFT yields from simulation at generator

inclusive cross sections
- simple EFT parameterization sufficient

re-interpretation of unfolded measurement → direct measurement from detector-level data

unfolded, differential cross sections
- parton or particle level
- needs differential MC EFT information

direct measurement of EFT
- no SM assumption
- consider EFT in all relevant processes
- perform simultaneous fit to multiple regions

- orthogonal to pure rate changes or enhancements in particle momentum spectrum
- high sensitivity to EFT, e.g. chromomagnetic top dipole moment (CMDM): c_{tG} O_{tG} with

$$O_{tG} = y_t g_s (\overline{Q}\sigma^{\mu\nu}T^a t)\tilde{\phi}G^a_{\mu\nu}$$

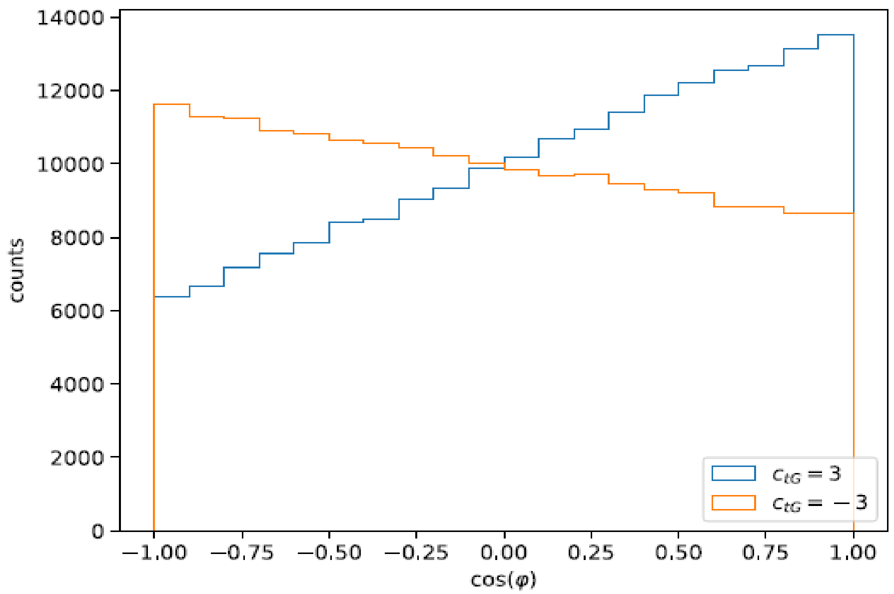

- 15 coefficients completely characterize spin dependence of $t\bar{t}$ production

$$\frac{1}{\sigma}\frac{d^4\sigma}{d\Omega_1 d\Omega_2} = \frac{1}{(4\pi)^2}\left(1 + \vec{B}_1\cdot\hat{\ell}^1 + \vec{B}_2\cdot\hat{\ell}^2 - \hat{\ell}^1\cdot C\cdot\hat{\ell}^2\right)$$

1 — spin-independent

$\vec{B}_{1/2} = \begin{pmatrix} x \\ x \\ x \end{pmatrix}$ — top polarization

$C = \begin{pmatrix} x & x & x \\ x & x & x \\ x & x & x \end{pmatrix}$ — spin correlation

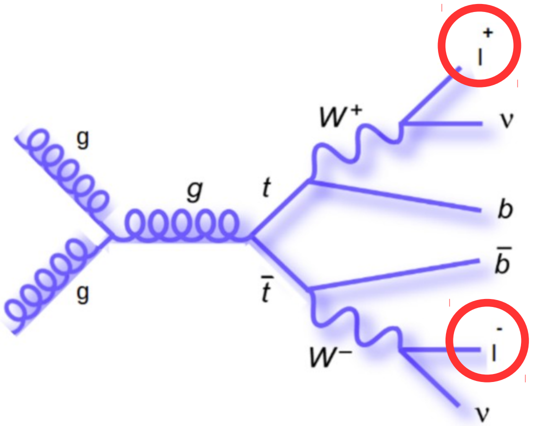

Analysis approach

- construct orthonormal basis

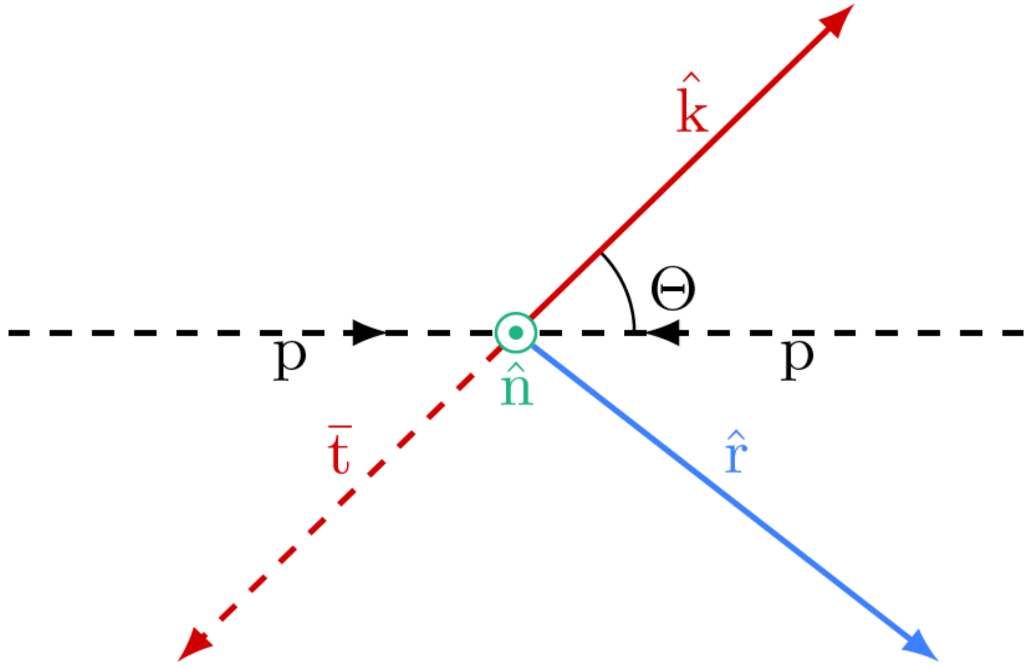

- construct orthonormal basis
- estimate angles in $t/\bar{t}$ rest frames → kinematic reconstruction

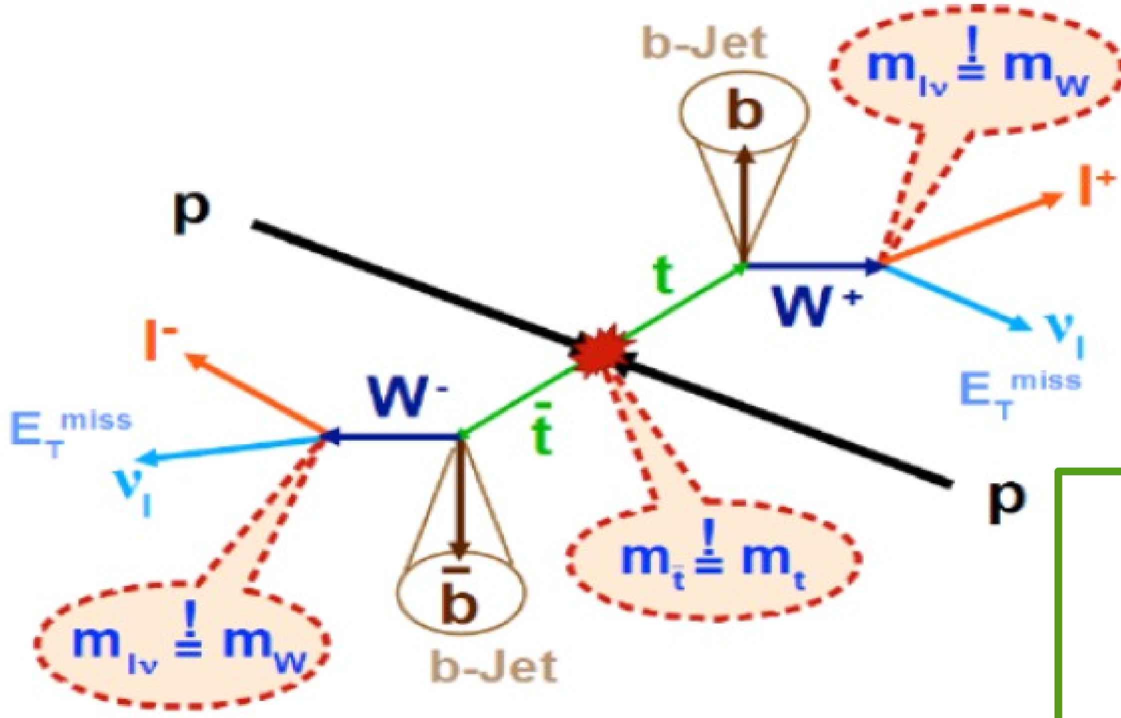

combination to pick

- solution with minimal $m_{t\bar{t}}$
- pair lepton and jet according to expected m_{lb}

Analysis approach

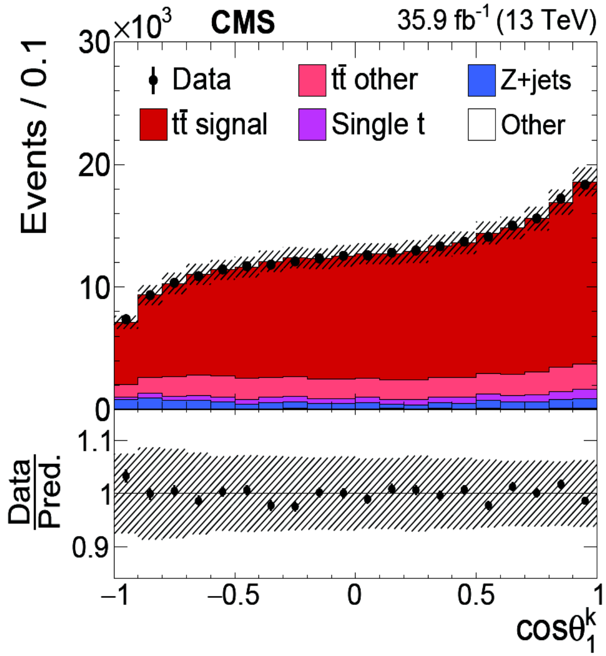

- construct orthonormal basis
- estimate angles in t/$\bar{t}$ rest frames → kinematic reconstruction

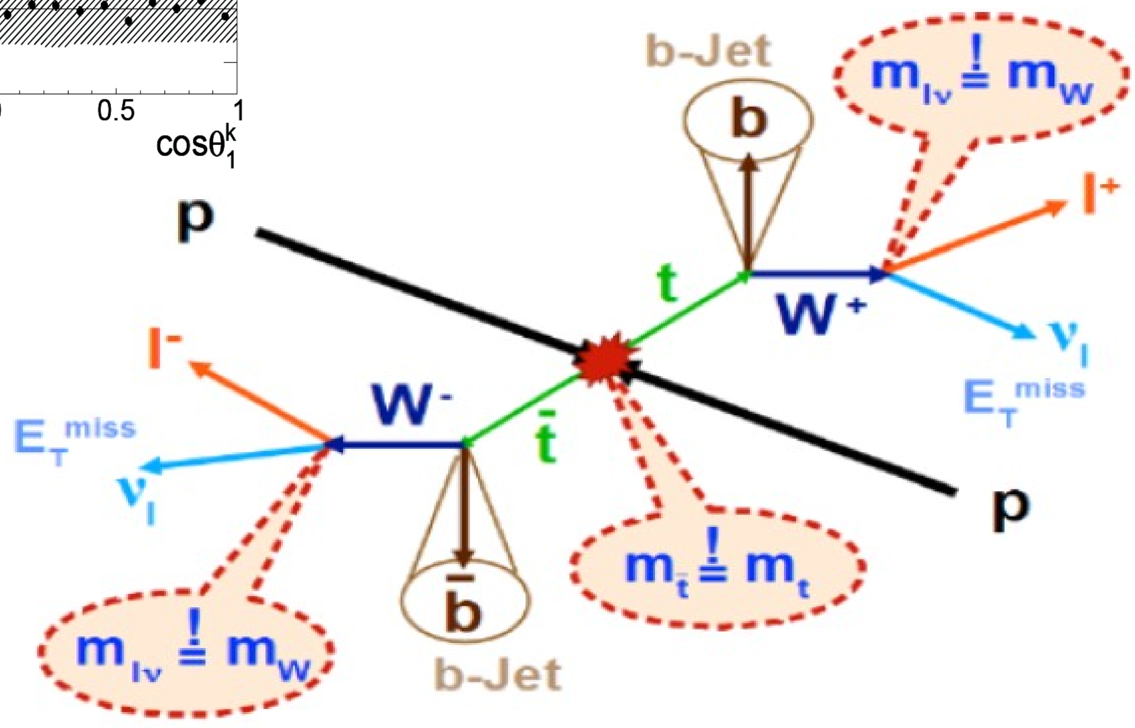

Analysis approach

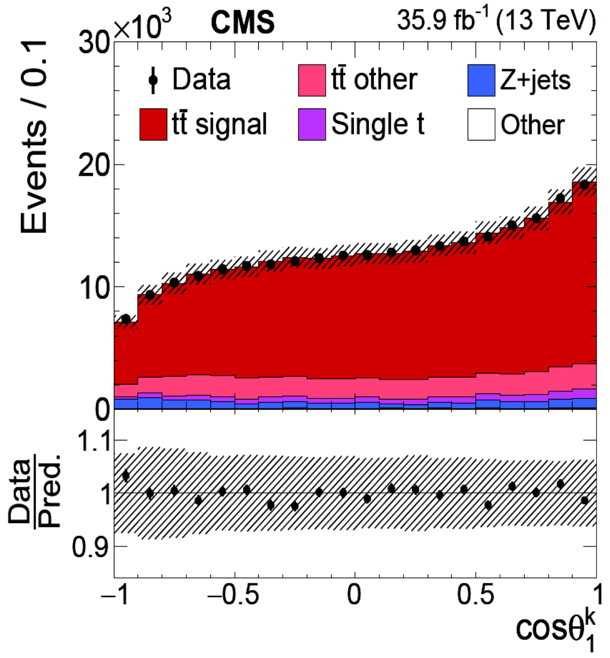

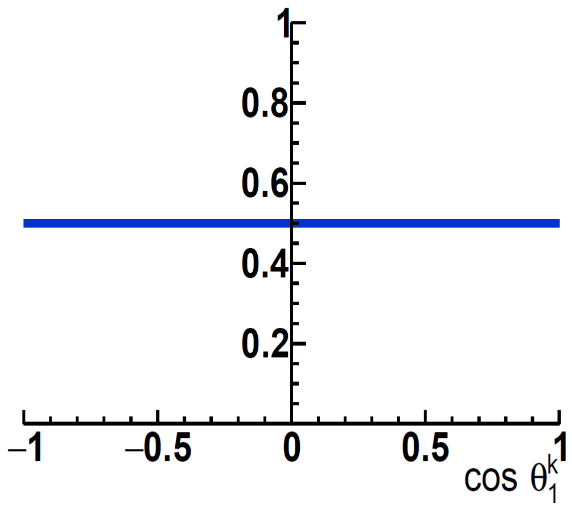

- construct orthonormal basis
- estimate angles in t/t̄ rest frames → kinematic reconstruction

Analysis approach

- construct orthonormal basis
- estimate angles in t/$\bar{t}$ rest frames → kinematic reconstruction
- correct acceptance and detector effects (parton-level unfolding)

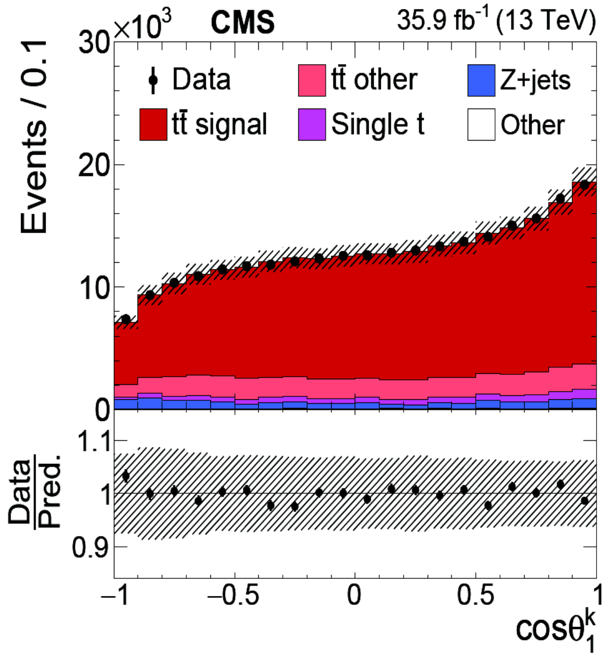

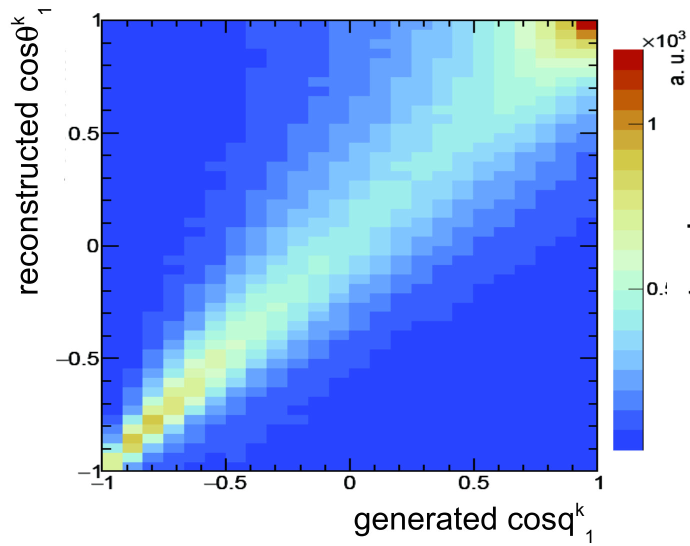

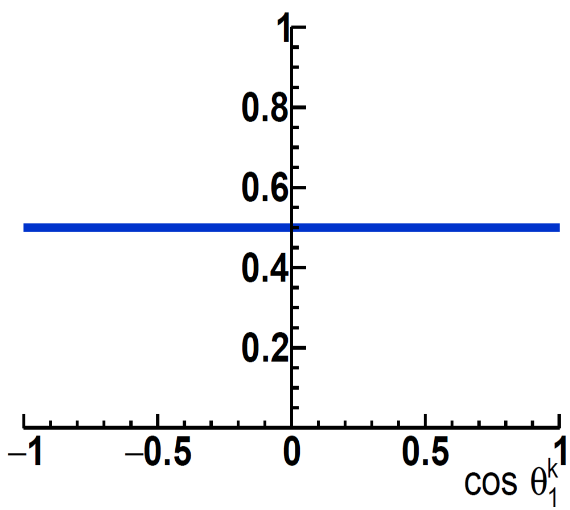

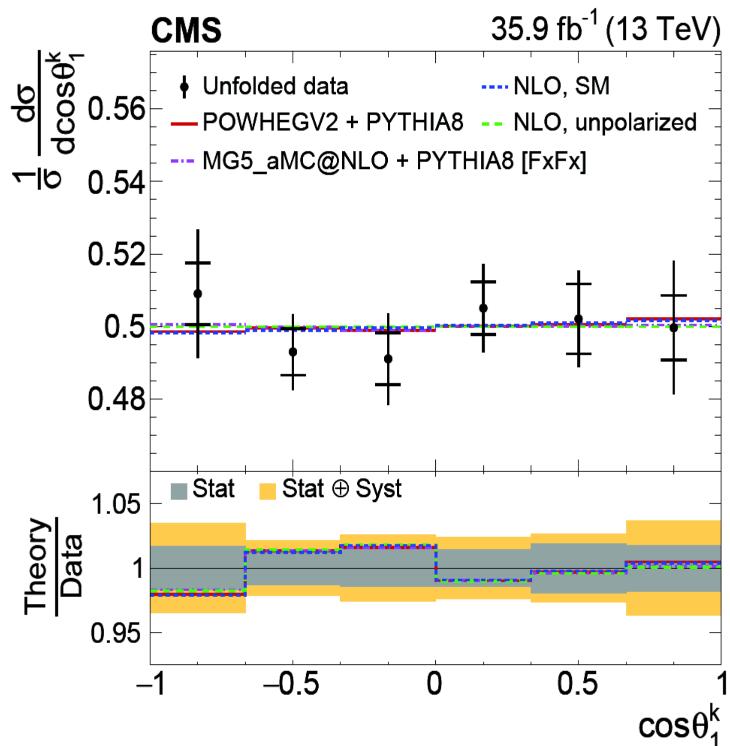

- consistent with zero for each axis
- not yet sensitive to small polarization in the SM
- dominant uncertainty from JES (top rest frame reconstruction)

$$\frac{1}{\sigma}\frac{d^4\sigma}{d\Omega_1 d\Omega_2} = \frac{1}{(4\pi)^2}\left(1 + \vec{B}_1 \cdot \hat{\ell}^1 + \vec{B}_2 \cdot \hat{\ell}^2 - \hat{\ell}^1 \cdot C \cdot \hat{\ell}^2\right)$$

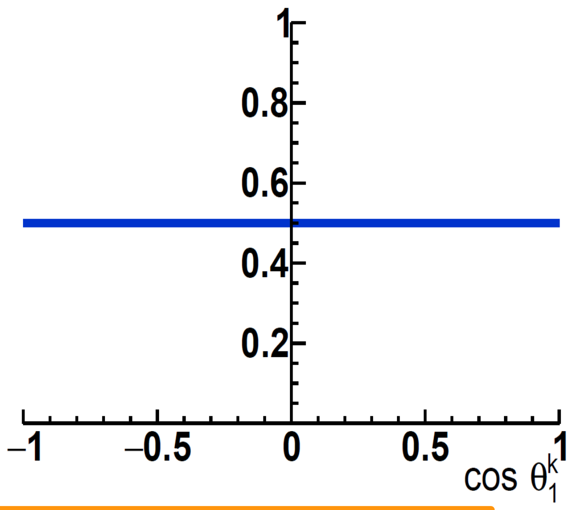

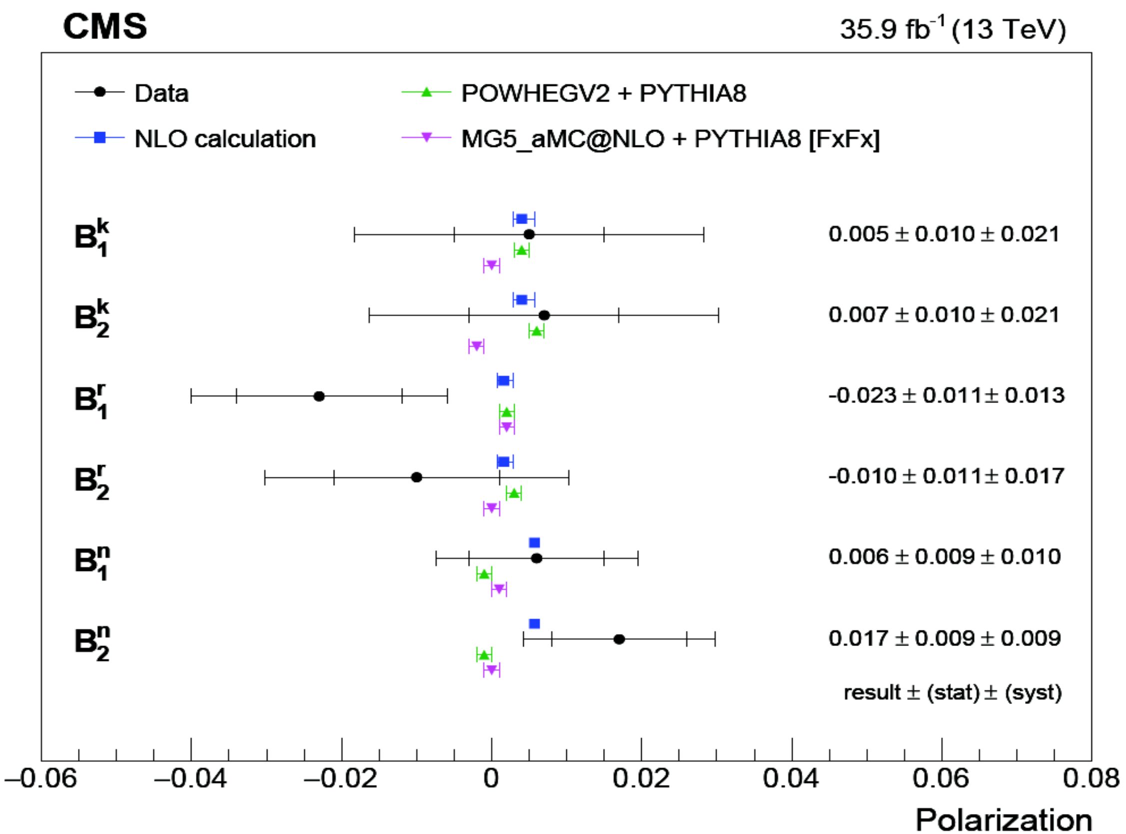

PRD 100 (2019) 072002

Results: diagonal correlation

- correlations along each axis consistent with SM expectations
- dominant uncertainties from background and top p_T modeling

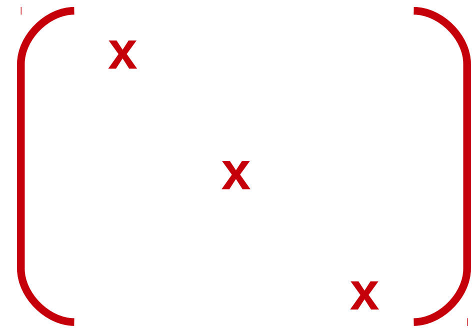

$$\frac{1}{\sigma}\frac{d^4\sigma}{d\Omega_1 d\Omega_2} = \frac{1}{(4\pi)^2}\left(1 + \vec{B}_1\cdot\hat{\ell}^1 + \vec{B}_2\cdot\hat{\ell}^2 - \hat{\ell}^1\cdot \mathrm{C}\cdot\hat{\ell}^2\right)$$

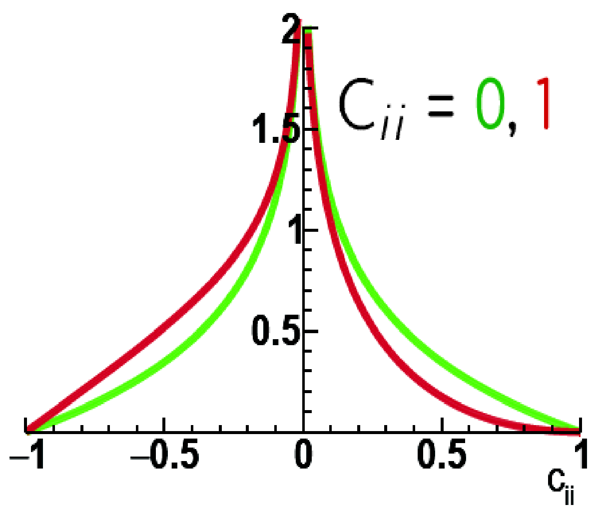

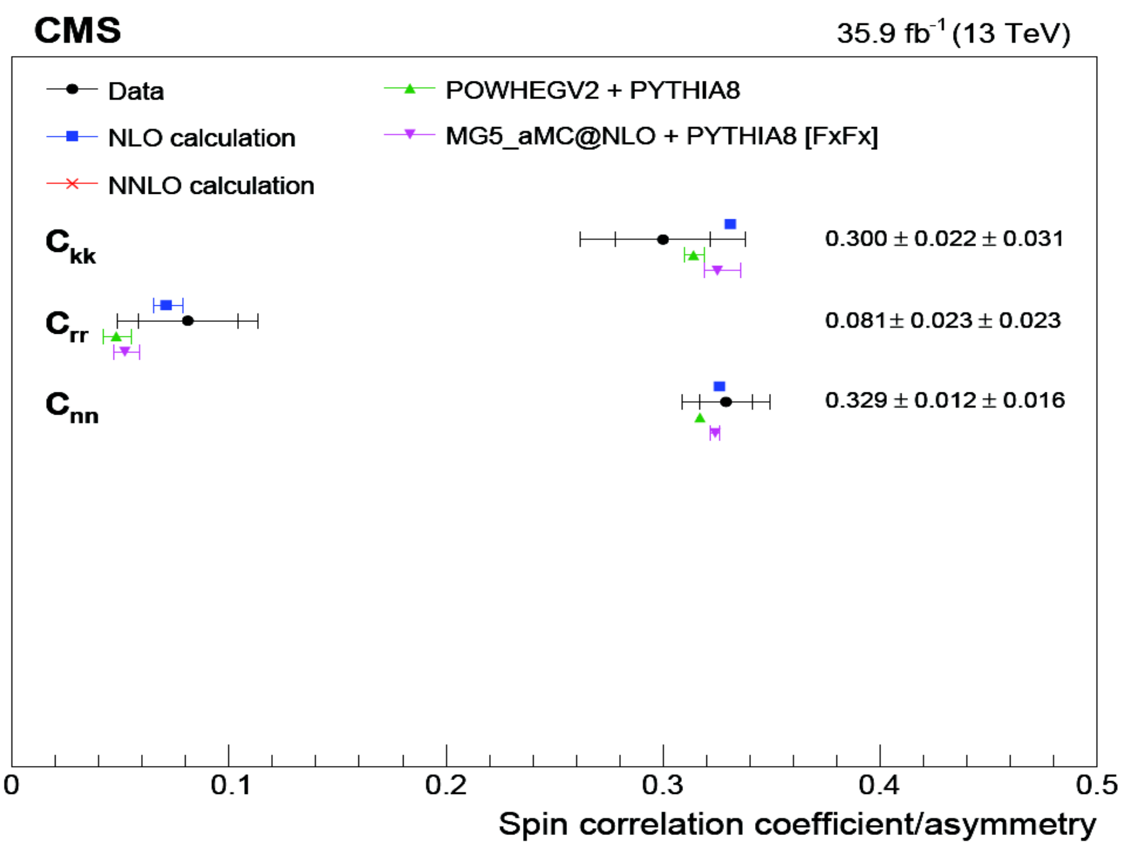

PRD 100 (2019) 072002

Maximal sensitivity to spin correlation

- provided by full lepton (in top parent rest frame) opening angle
- most precise measurement to date (5% uncertainty)

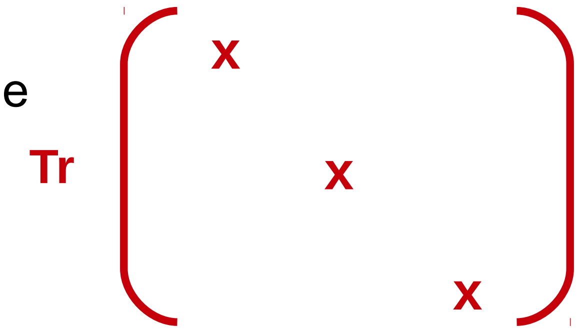

$$\frac{1}{\sigma}\frac{d^4\sigma}{d\Omega_1 d\Omega_2} = \frac{1}{(4\pi)^2}\left(1 + \vec{B}_1 \cdot \hat{\ell}^1 + \vec{B}_2 \cdot \hat{\ell}^2 - \hat{\ell}^1 \cdot C \cdot \hat{\ell}^2\right)$$

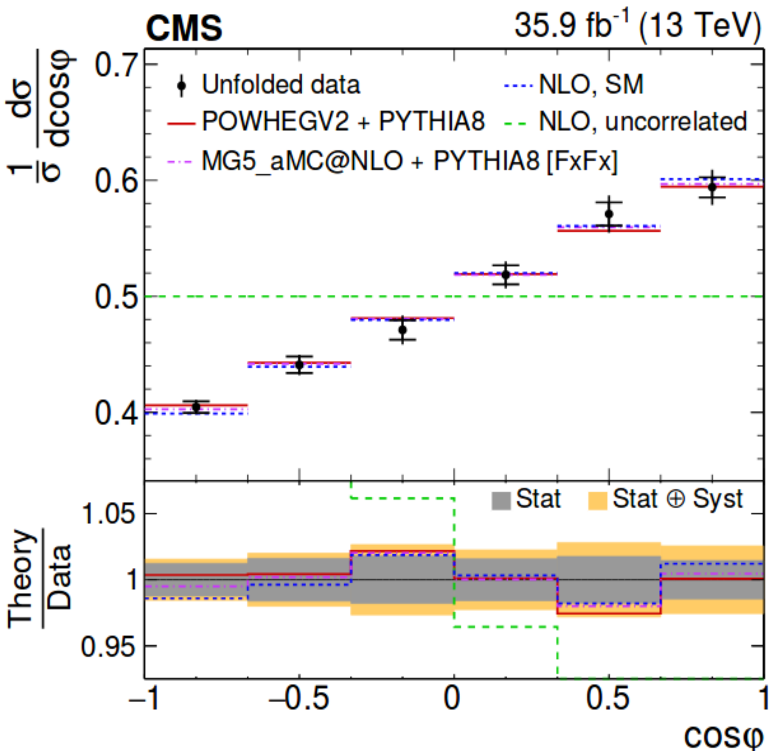

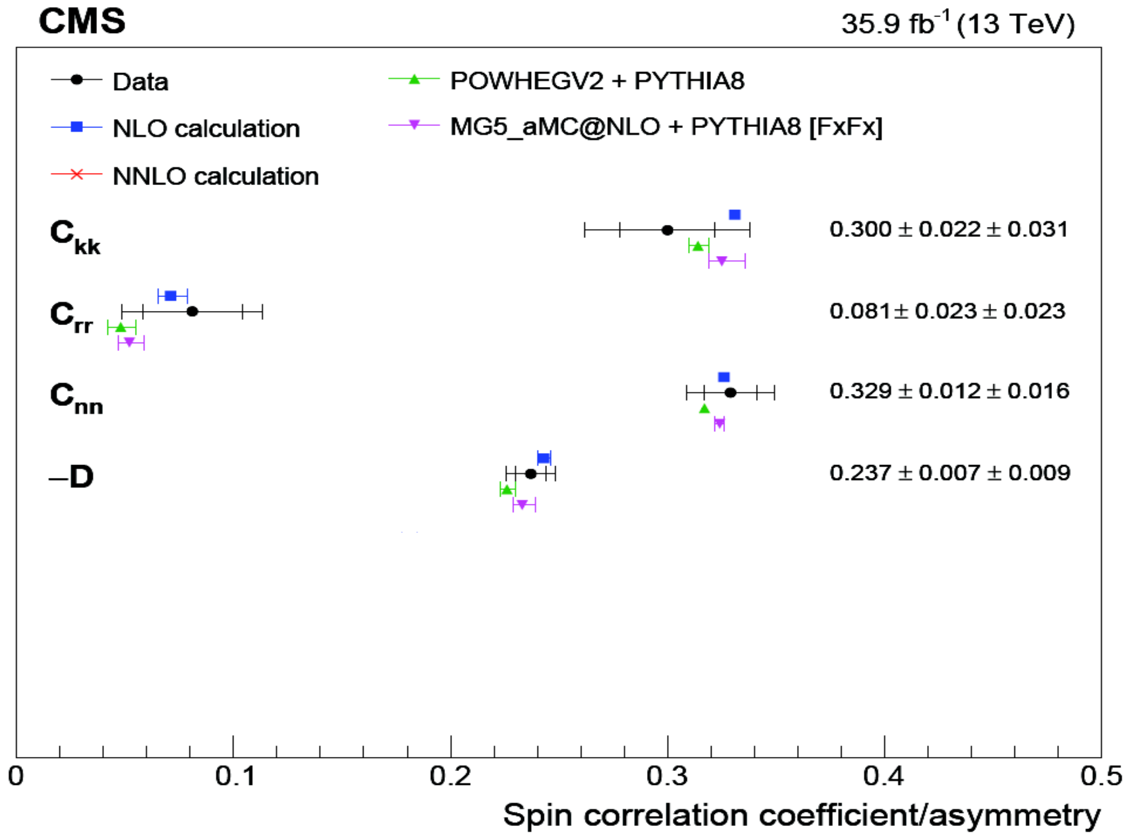

PRD 100 (2019) 072002

Constraining top chromomagnetic dipole moment

$$O_{tG} = y_t g_s (\bar{Q}\sigma^{\mu\nu}T^a t)\tilde{\phi}G^a_{\mu\nu}$$

- EFT predictions based on NLO MC simulation
  - apply NNLO/NLO k-factor of 1.22 from SM calculation

- 95% CL limits from simultaneous χ^2 fit
  - to normalized cos(φ), C_{kk}, C_{nn}, C_{rk} + C_{kr}
  - including full covariance matrix V_{ij}

$$\chi^2 = \sum_i^N \sum_j^N \left(\text{data}_i - \text{pred}_i\right) \cdot \left(\text{data}_j - \text{pred}_j\right) \cdot V_{ij}^{-1}$$

- strongest direct limits to date on top quark CMDM

$-0.10 < C_{tG}/\Lambda^2 < 0.22$ TeV^{-2}

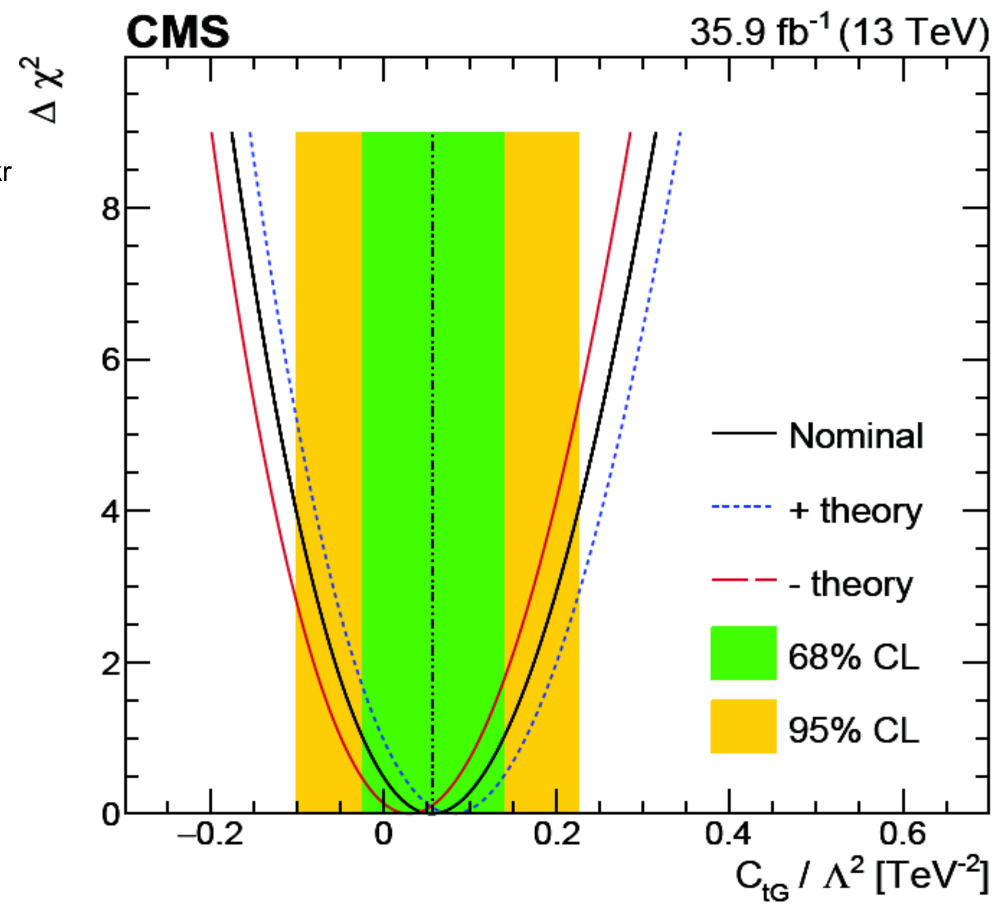

PRD 100 (2019) 072002

Beyond top CMDM

- total of 11 EFT operators affecting hadronic $t\bar{t}$ production
  - 10 of them impact spin density matrix (LO prediction from JHEP 12 (2015) 026)
  - choose 4 best observables to constraint each operator

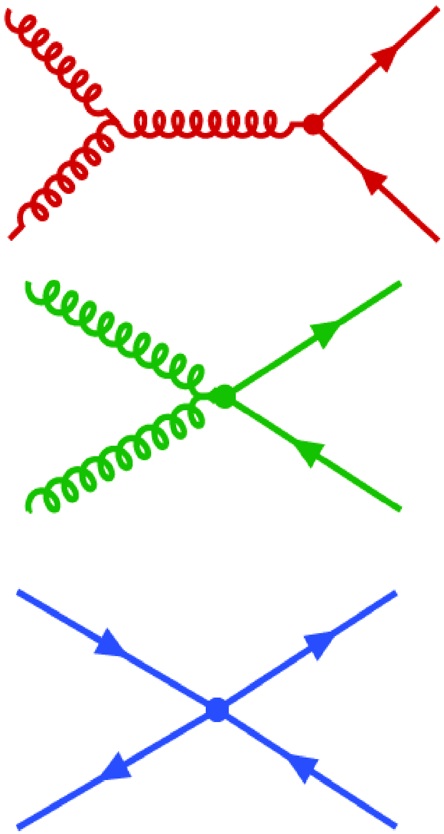

Operator	Lagrangian	Vertex	Direct effects
$\hat{\mu}_t$	$g_1 [\bar{t}\sigma^{\mu\nu}T^a t G^a_{\mu\nu}]$	$gt\bar{t}$ $ggt\bar{t}$	C_{ii}, $C_{rk}+C_{kr}$, C_{hel}
$\hat{d}_t$	$g_1 [\bar{t}i\sigma^{\mu\nu}\gamma_5 T^a t G^a_{\mu\nu}]$	$gt\bar{t}$ $ggt\bar{t}$	$C_{nr}-C_{rn}$, $C_{nk}-C_{kn}$
$\hat{c}_{--}$	$g_2 [\mathcal{O}_- + \mathcal{O}_-^\dagger]$, $\mathcal{O}_- = i[\bar{t}\gamma^\mu\gamma_5 T^a D^\nu t]G^a_{\mu\nu}$	$ggt\bar{t}$	$C_{nr}-C_{rn}$, $C_{nk}-C_{kn}$
$\hat{c}_{-+}$	$g_2 i [\mathcal{O}_+ - \mathcal{O}_+^\dagger]$, $\mathcal{O}_+ = [\bar{t}\gamma^\mu T^a D^\nu t]G^a_{\mu\nu}$	$ggt\bar{t}$	b^a_n
$\hat{c}_{VV}$	$g_3 q_V t_V$	$q\bar{q}t\bar{t}$	C_{ii}, $C_{rk}+C_{kr}$, C_{hel}
$\hat{c}_{VA}$	$g_3 q_V t_A$ weak isospin 0	$q\bar{q}t\bar{t}$	b^a_k, b^a_r
$\hat{c}_{AV}$	$g_3 q_A t_V$	$q\bar{q}t\bar{t}$	$b^a_{k^*}$, $b^a_{r^*}$
$\hat{c}_{AA}$	$g_3 q_A t_A$	$q\bar{q}t\bar{t}$	-
$\hat{c}_1$	$g_4 [q'_V t_V + q'_A t_V]$	$q\bar{q}t\bar{t}$	C_{ii}, $C_{rk}+C_{kr}$, C_{hel}
$\hat{c}_3$	$g_4 [q'_V t_A + q'_A t_V]$ weak isospin 1	$q\bar{q}t\bar{t}$	b^a_k, b^a_r
$\hat{c}_1 - \hat{c}_2 + \hat{c}_3$	$\hat{c}_2 = g_4 [q'_A t_A - q'_A t_V]$	$q\bar{q}t\bar{t}$	$b^a_{k^*}$, $b^a_{r^*}$

definition following JHEP 12 (2015) 026
table by A. Anuar

- total of 11 EFT operators affecting hadronic $t\bar{t}$ production
  - 10 of them impact spin density matrix (LO prediction from JHEP 12 (2015) 026)
  - choose 4 best observables to constraint each operator

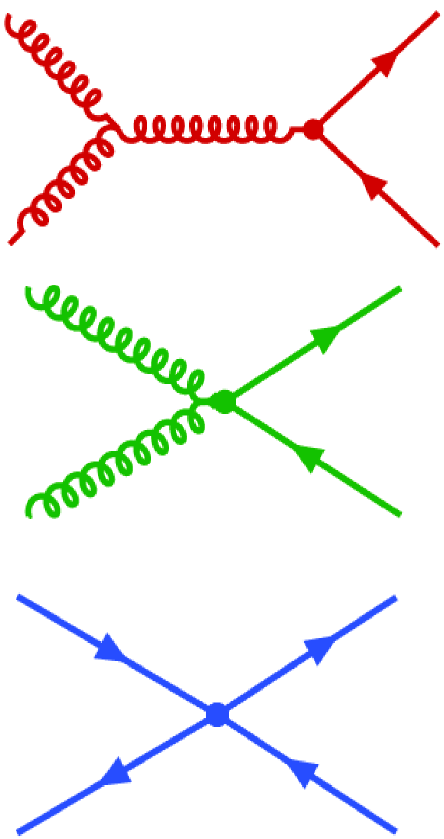

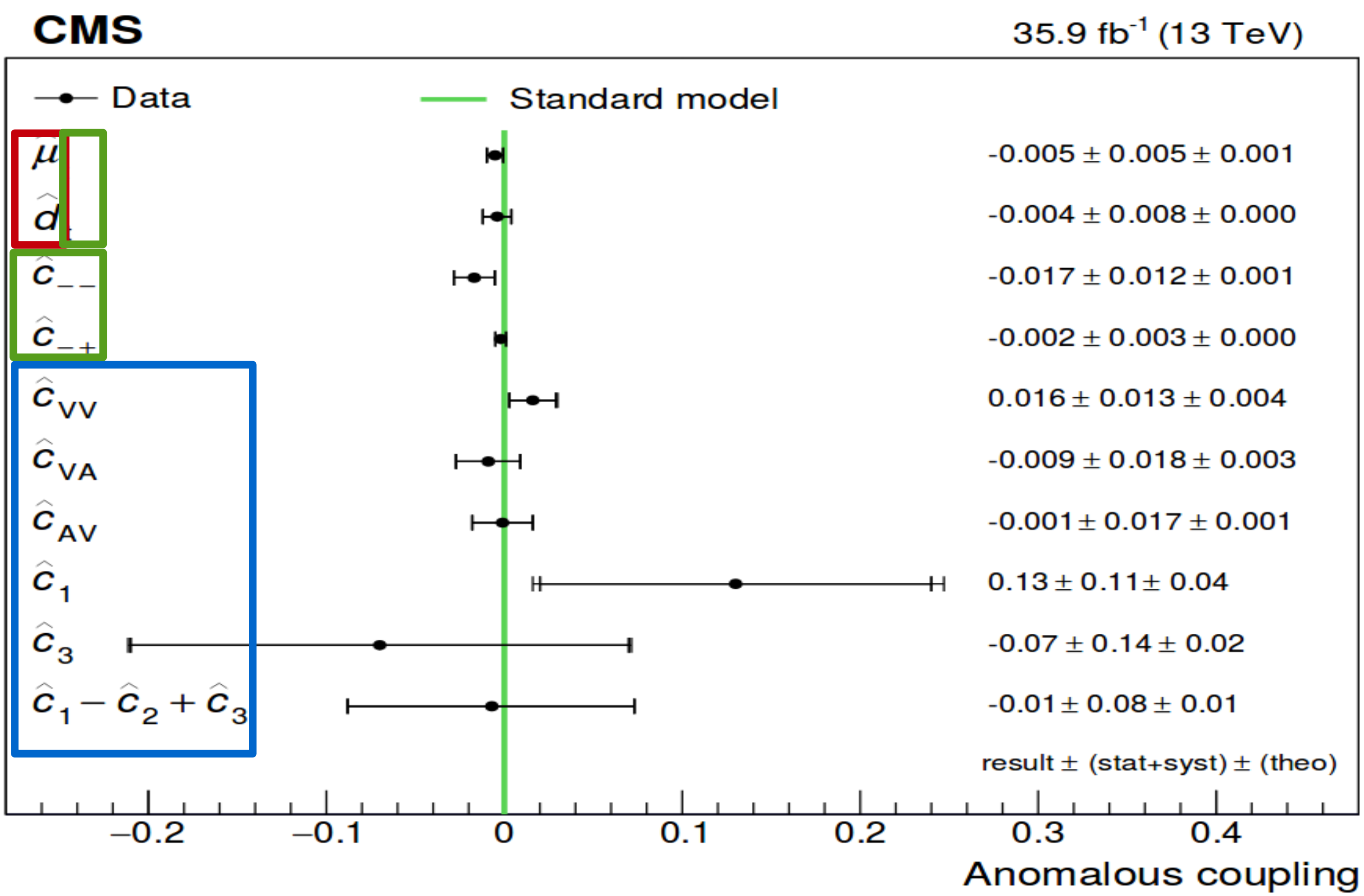

PRD 100 (2019) 072002

Beyond top CMDM

- total of 11 EFT operators affecting hadronic $t\bar{t}$ production
  - 10 of them impact spin density matrix (LO prediction from JHEP 12 (2015) 026)
  - choose 4 best observables to constraint each operator
  - 2 dimensional contours provided where needed

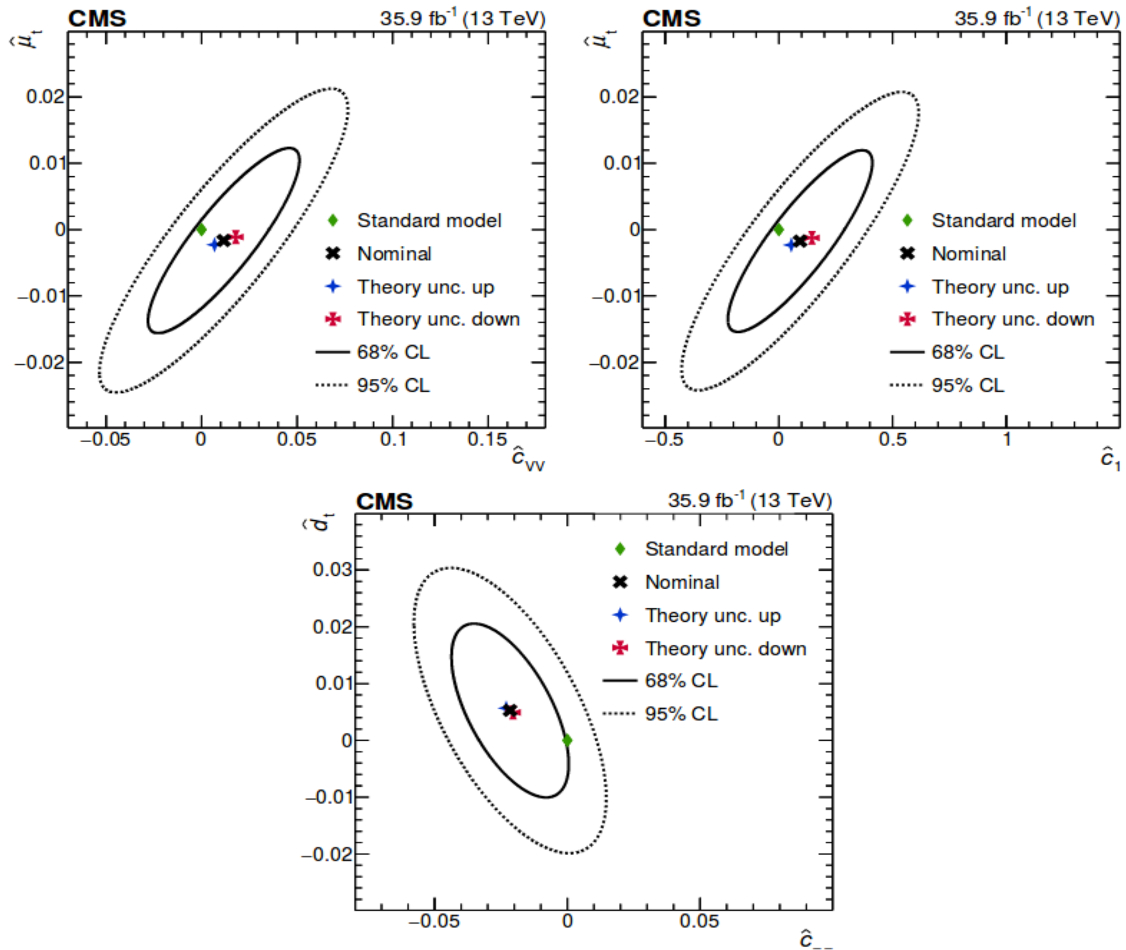

PRD 100 (2019) 072002

Zooming in on $q\bar{q}t\bar{t}$

- $q\bar{q} \rightarrow t\bar{t}$ production asymmetric at NLO due to interferences

pos. asymmetry

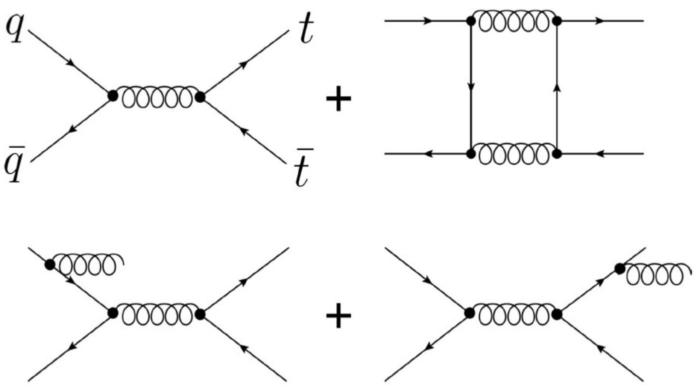

neg. asymmetry

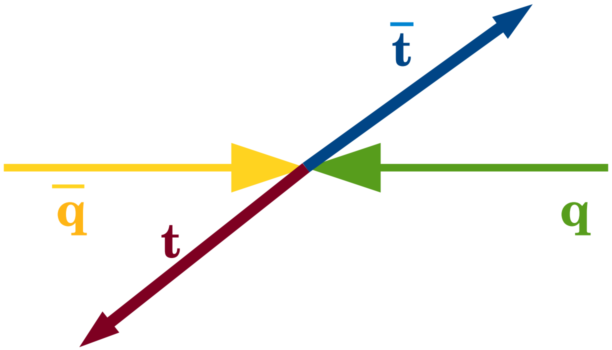

- $q\bar{q} \rightarrow t\bar{t}$ production asymmetric at NLO due to interferences

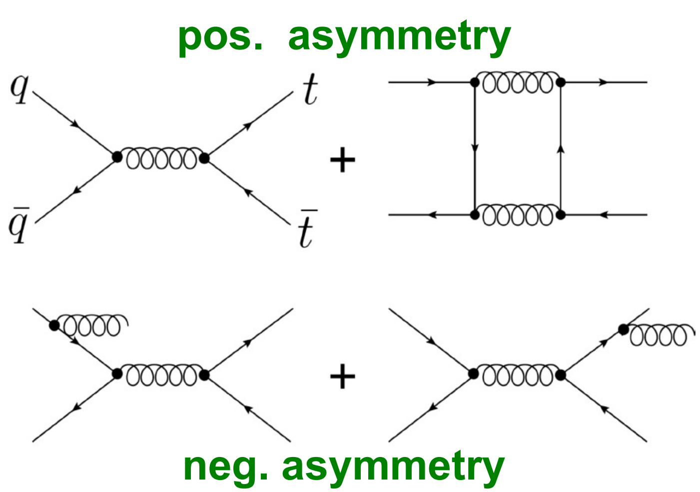

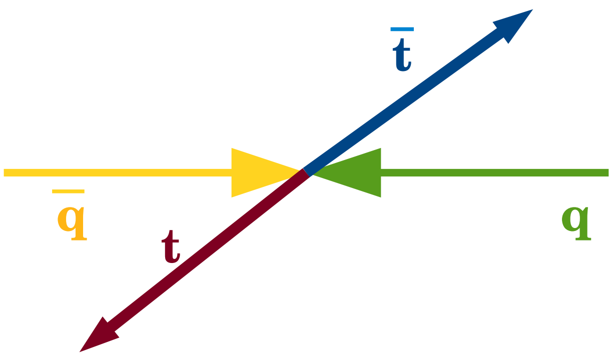

- quark momentum on average higher in pp collision

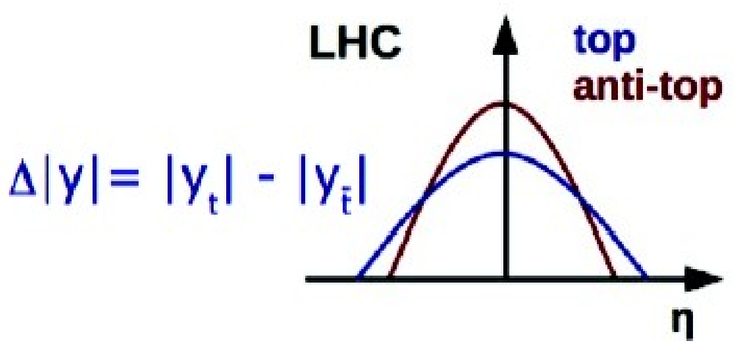

$$A_C = \frac{N(\Delta|y_{t\bar{t}}|>0) - N(\Delta|y_{t\bar{t}}|<0)}{N(\Delta|y_{t\bar{t}}|>0) + N(\Delta|y_{t\bar{t}}|<0)}$$

use A_c to probe $q\bar{q}t\bar{t}$ vertex

- consider linear combinations, e.g. for up quarks

$$O_{qq}^{(8,1)} = \tfrac{1}{4}(\bar{q}^i \gamma_\mu \lambda^A q^j)(\bar{q}\gamma^\mu \lambda^A q)$$
$$O_{qq}^{(8,3)} = \tfrac{1}{4}(\bar{q}^i \gamma_\mu \tau^I \lambda^A q^j)(\bar{q}\gamma^\mu \tau^I \lambda^A q)$$
$$O_{ut}^{(8)} = \tfrac{1}{4}(\bar{u}^i \gamma_\mu \lambda^A u^j)(\bar{t}\gamma^\mu \lambda^A t)$$

$$C_u^1 = C_{qq}^{(8,1)} + C_{qq}^{(8,3)} + C_{ut}^{(8)}$$
$$C_u^2 = C_{qu}^{(1)} + C_{qt}^{(1)}$$

$$O_{qt}^{(1)} = (\bar{q}^i t)(\bar{t} q^j)$$
$$O_{qu}^{(1)} = (\bar{q} u^i)(\bar{u}^j q)$$

- assume equal couplings to up and down quarks
  - $C_u^1 = C_d^1 = C^1$
  - $C_u^2 = C_d^2 = C^2$
- complementary to $t\bar{t}$ cross section
  - $\sigma_{t\bar{t}} - \sigma_{t\bar{t}}^{SM} \sim C^1 + C^2$
  - $A_c - A_c^{SM} \sim C_u^1 - C^2$

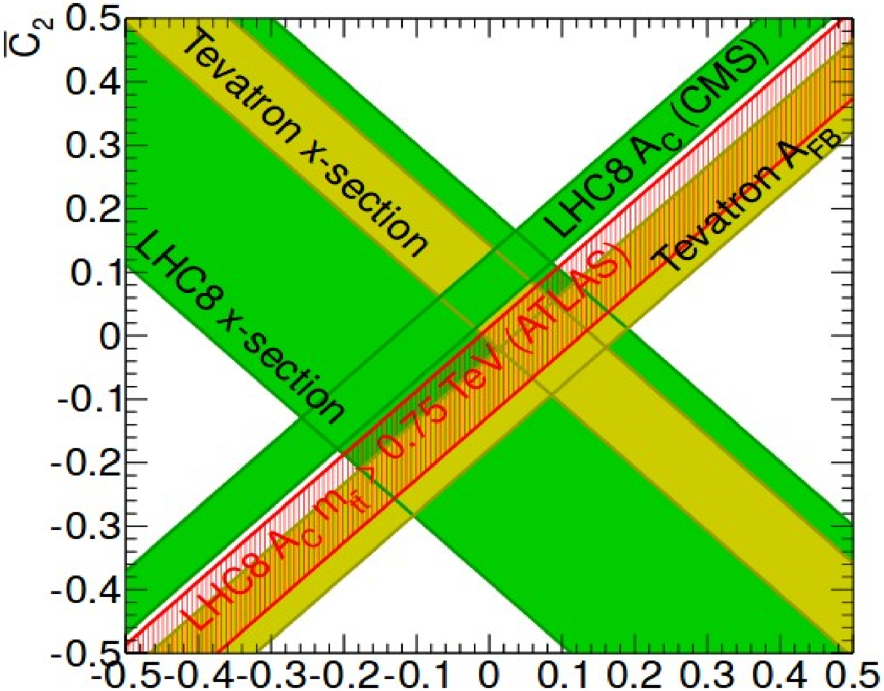

arXiv: 1512.07542

A_c analysis strategy

- reconstruct $t\bar{t}$ event in case of 4 jets and 1 lepton ("resolved")
  - use BDT with 13 variables to find correct jet-parton combination: 75% efficiency

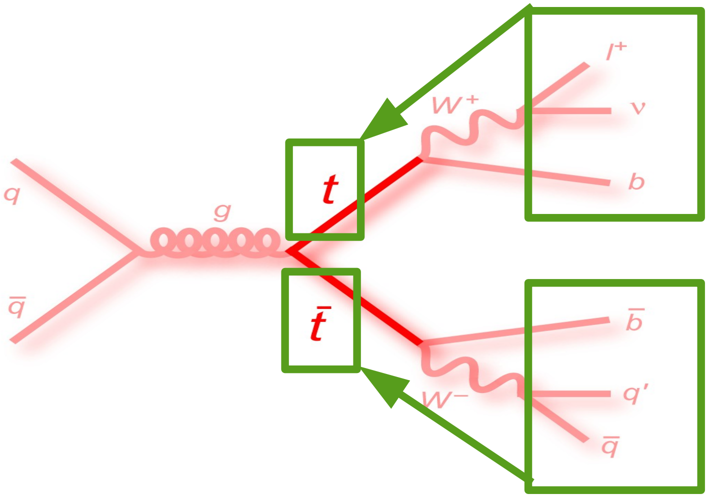

- reconstruct $t\bar{t}$ event in case of 4 jets and 1 lepton ("resolved")
  - use BDT with 13 variables to find correct jet-parton combination: 75% efficiency

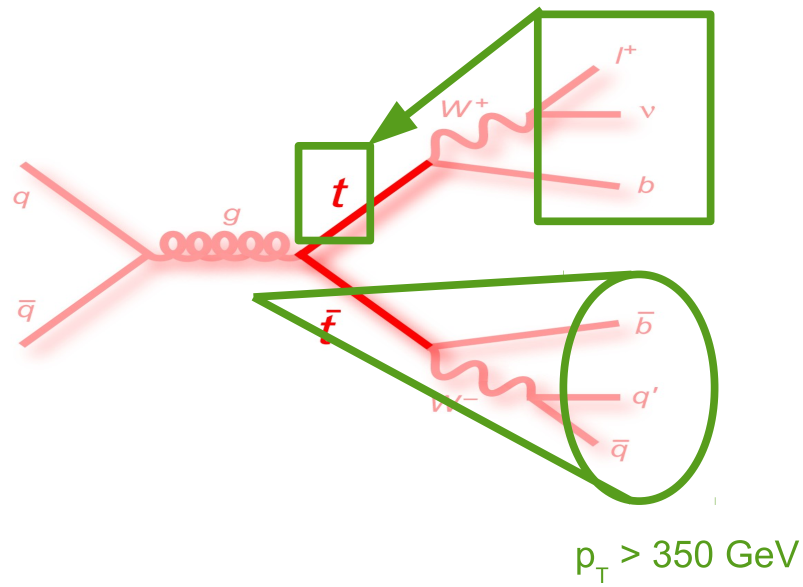

- add events with one top-tagged R=1 anti-kt jet, 1 lepton and 1 small jet ("boosted")

- reconstruct $t\bar{t}$ event in case of 4 jets and 1 lepton (“resolved”)
  - use BDT with 13 variables to find correct jet-parton combination: 75% efficiency

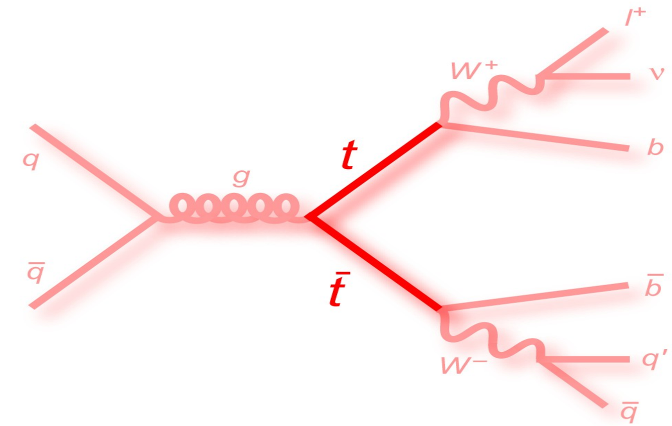

- add events with one top-tagged R=1 anti-kt jet, 1 lepton and 1 small jet (“boosted”)

- use fully Bayesian unfolding
  - correcting for acceptance and resolution
  - bring Δ|y| back to top parton-level
  - marginalization benefits from large data set

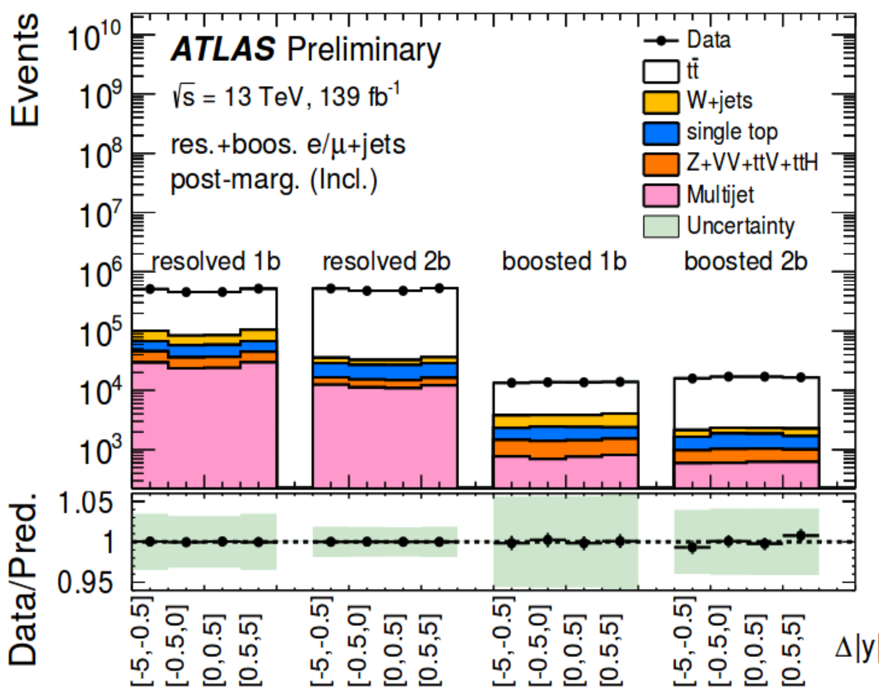

Extracting A_c

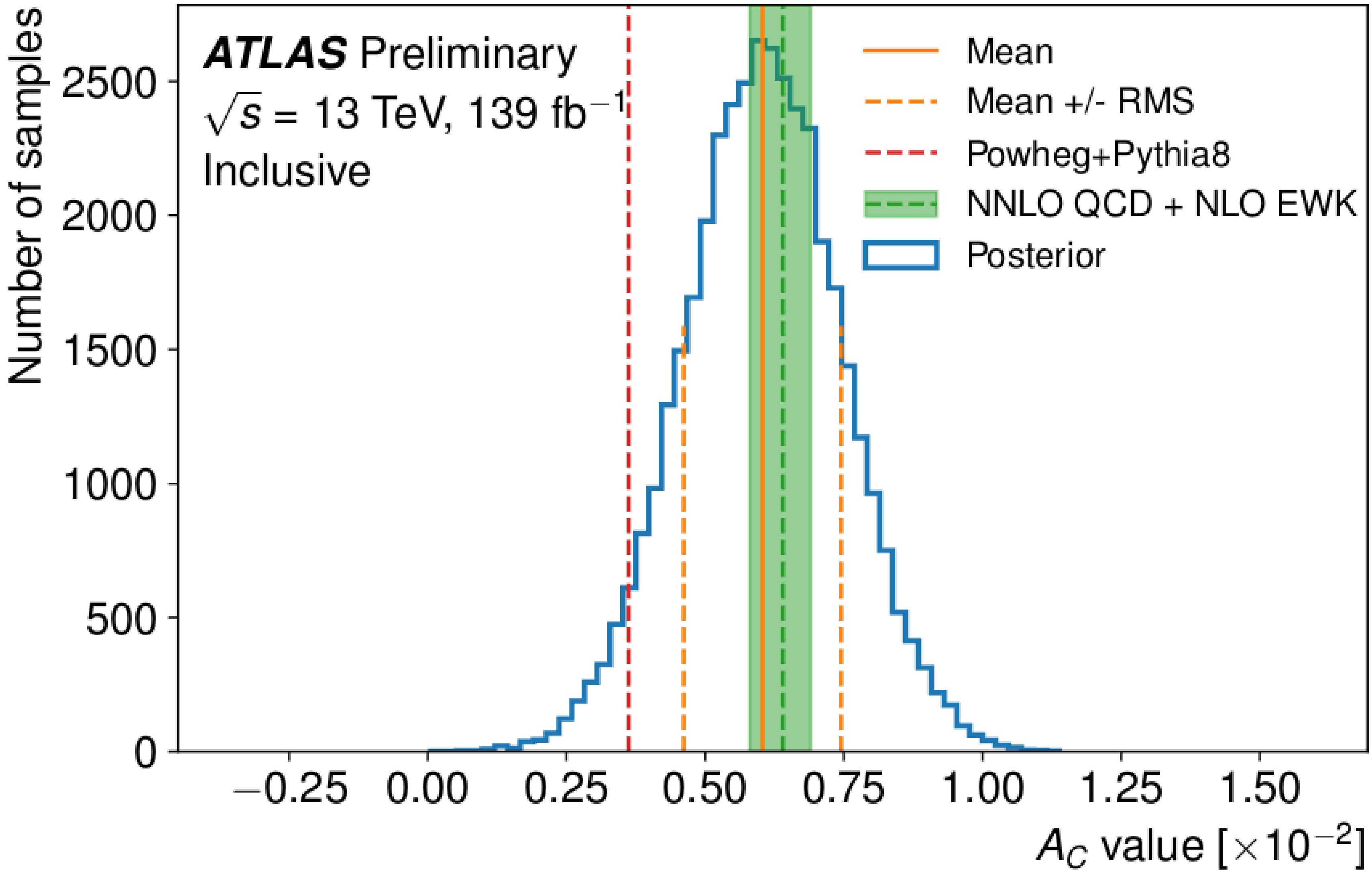

ATLAS-CONF-2019-026

inclusive result well consistent with SM expectation
0.0060 ± 0.0015

A_c as a function of $m_{t\bar{t}}$

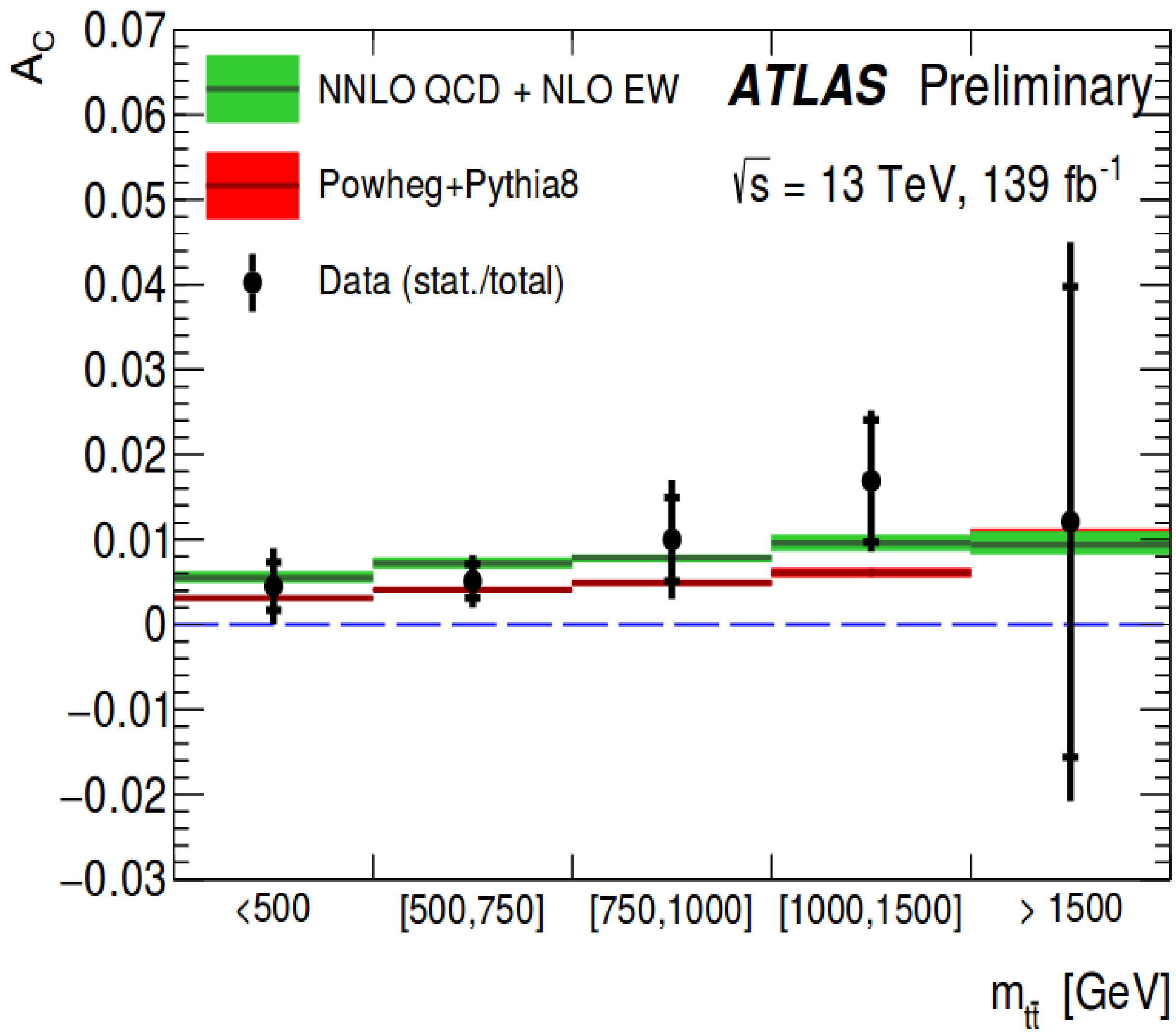

ATLAS-CONF-2019-026

enhance BSM sensitivity by going differentially

Turning A_c into limits on 2light-2heavy operators

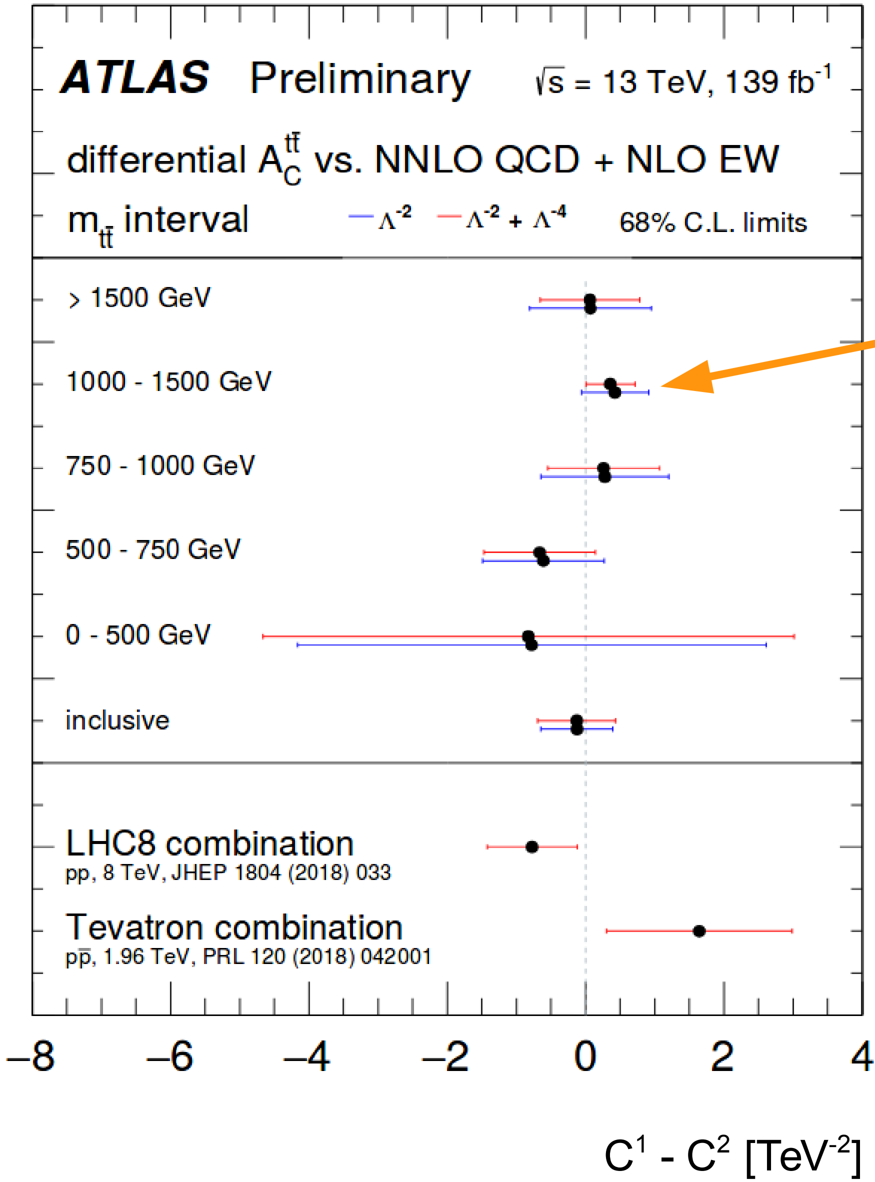

best trade off between $m_{t\bar{t}}$ EFT enhancement and A_c precision

ATLAS-CONF-2019-026

good improvement over previous results

EFT Approaches in ATLAS and CMS

hybrid measurement at detector-level

- (SM+EFT)/SM reweighting at generator-level, direct comparison to data
- take SM shape, estimate SM+EFT yields from simulation at generator

inclusive cross sections

- simple EFT parameterization sufficient

re-interpretation of unfolded measurement → direct measurement from detector-level data

unfolded, differential cross sections

- parton or particle level
- needs differential MC EFT information

direct measurement of EFT

- no SM assumption
- consider EFT in all relevant processes
- perform simultaneous fit to multiple regions

Measuring top-Z couplings

- electroweak-top interactions from $t\bar{t}Z$ production
  - split events with 3/4 leptons into jet/b-jet multiplicity bins

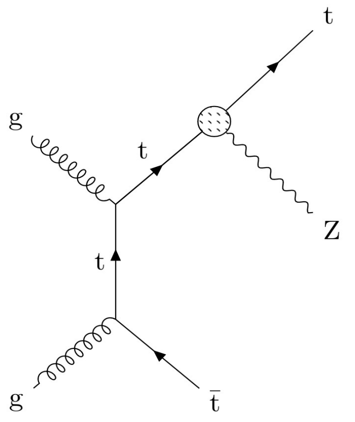

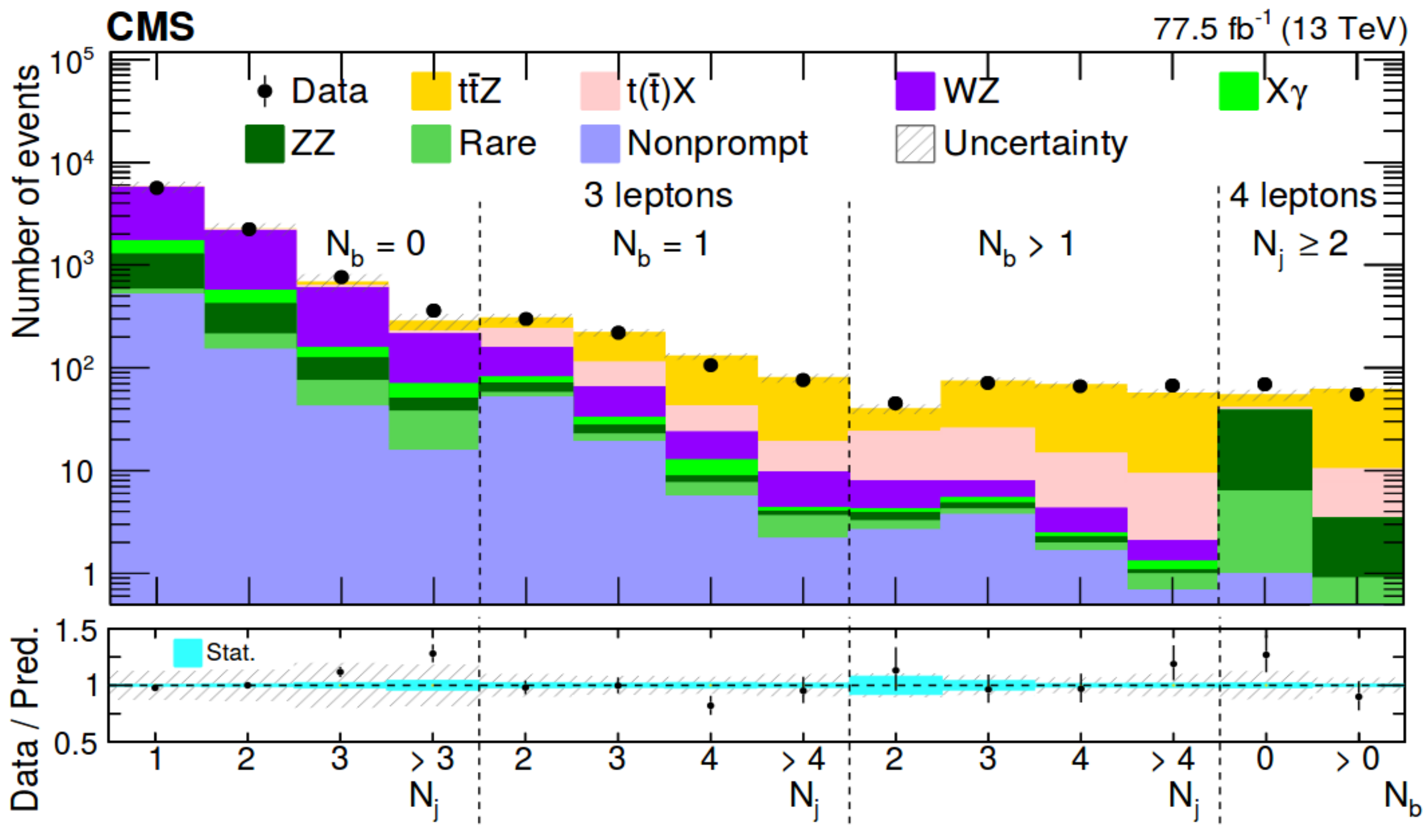

Measuring top-Z couplings

- electroweak-top interactions from $t\bar{t}Z$ production
- translate cross-section measurements into limits
  - 4 independent EFT operators

$$c_{tZ} = \mathrm{Re}\left(-\sin\theta_W C_{uB}^{(33)} + \cos\theta_W C_{uW}^{(33)}\right)$$
$$c_{tZ}^{[I]} = \mathrm{Im}\left(-\sin\theta_W C_{uB}^{(33)} + \cos\theta_W C_{uW}^{(33)}\right)$$
$$c_{\phi t} = C_{\phi t} = C_{\phi u}^{(33)}$$
$$c_{\phi Q}^{-} = C_{\phi Q} = C_{\phi q}^{1(33)} - C_{\phi q}^{3(33)}$$

≡ 0 : assume SM Wtb vertex

tensor couplings (quad.): $C_{tZ}/C_{tZ}^{[I]}$

$$O_{uB}^{(ij)} = (\bar{q}_i \sigma^{\mu\nu} u_j) \quad \tilde{\varphi} B_{\mu\nu}$$
$$O_{uW}^{(ij)} = (\bar{q}_i \sigma^{\mu\nu} \tau^I u_j)\, \tilde{\varphi} W_{\mu\nu}^I$$

vector couplings (lin.): $C_{\Phi t}/C^{-}_{\Phi Q}$

$$O_{\varphi u}^{(ij)} = (\varphi^\dagger i\overleftrightarrow{D}_\mu \varphi)(\bar{u}_i \gamma^\mu u_j)$$
$$O_{\varphi q}^{1(ij)} = (\varphi^\dagger i\overleftrightarrow{D}_\mu \varphi)(\bar{q}_i \gamma^\mu q_j)$$
$$O_{\varphi q}^{3(ij)} = (\varphi^\dagger i\overleftrightarrow{D}_\mu^I \varphi)(\bar{q}_i \gamma^\mu \tau^I q_j)$$

- electroweak-top interactions from $t\bar{t}Z$ production

- translate cross-section measurements into limits
  - 4 independent EFT operators
  - main impact on p_T^Z and $\cos(\Phi_Z^*)$ → use to reweight NLO SM simulations

$$c_{tZ} = \mathrm{Re}\left(-\sin\theta_W C_{uB}^{(33)} + \cos\theta_W C_{uW}^{(33)}\right)$$
$$c_{tZ}^{[I]} = \mathrm{Im}\left(-\sin\theta_W C_{uB}^{(33)} + \cos\theta_W C_{uW}^{(33)}\right)$$
$$c_{\phi t} = C_{\phi t} = C_{\phi u}^{(33)}$$
$$c_{\phi Q}^{-} = C_{\phi Q} = C_{\phi q}^{1(33)}$$

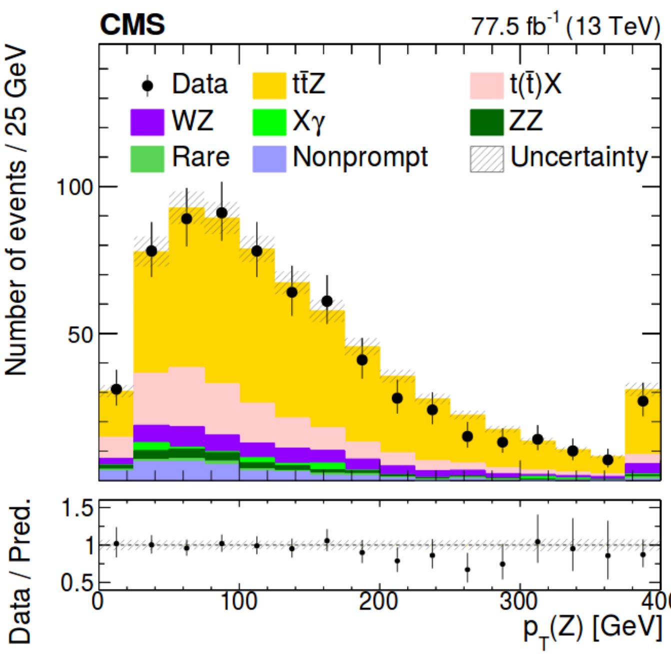

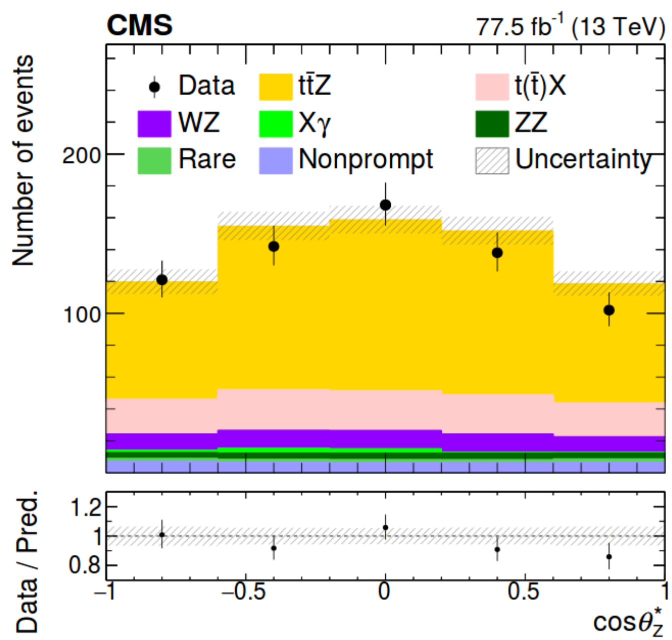

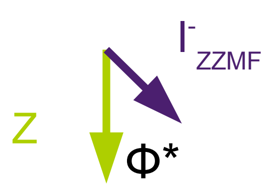

tensor couplings (quad.): $C_{tZ}/C_{tZ}^{[I]}$

$$O_{uB}^{(ij)} = (\bar{q}_i \sigma^{\mu\nu} u_j) \quad \tilde{\varphi} B_{\mu\nu}$$
$$O_{uW}^{(ij)} = (\bar{q}_i \sigma^{\mu\nu} \tau^I u_j)\, \tilde{\varphi} W_{\mu\nu}^I$$

vector couplings (lin.): $C_{\Phi t}/C^{-}_{\Phi Q}$

$$O_{\varphi u}^{(ij)} = (\varphi^\dagger i\overleftrightarrow{D}_\mu \varphi)(\bar{u}_i \gamma^\mu u_j)$$
$$O_{\varphi q}^{1(ij)} = (\varphi^\dagger i\overleftrightarrow{D}_\mu \varphi)(\bar{q}_i \gamma^\mu q_j)$$
$$O_{\varphi q}^{3(ij)} = (\varphi^\dagger i\overleftrightarrow{D}_\mu^I \varphi)(\bar{q}_i \gamma^\mu \tau^I q_j)$$

- electroweak-top interactions from $t\bar{t}Z$ production
- translate cross-section measurements into limits
- additional bins of p_T^Z and $\cos(\Phi_Z^*)$ for enhanced sensitivity

$$\begin{aligned}
c_{tZ} &= \mathrm{Re}\left(-\sin\theta_W C_{uB}^{(33)} + \cos\theta_W C_{uW}^{(33)}\right) \\
c_{tZ}^{[I]} &= \mathrm{Im}\left(-\sin\theta_W C_{uB}^{(33)} + \cos\theta_W C_{uW}^{(33)}\right) \\
c_{\phi t} &= C_{\phi t} = C_{\phi u}^{(33)} \\
c_{\phi Q}^{-} &= C_{\phi Q} = C_{\phi q}^{1(33)}
\end{aligned}$$

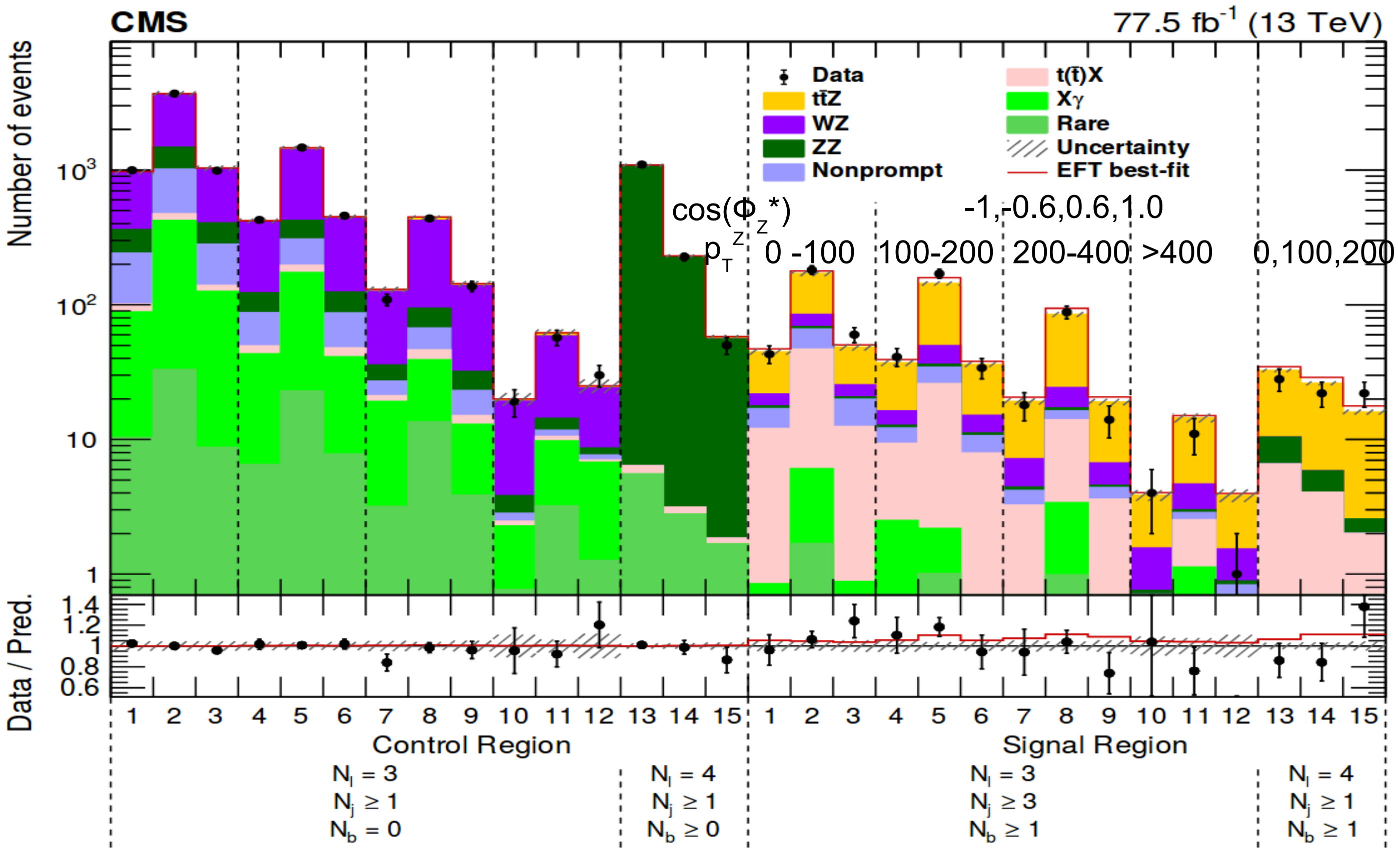

Limits on anomalous top-Z couplings

20% reduction from $p_T^Z/\cos(\Phi_Z^*)$

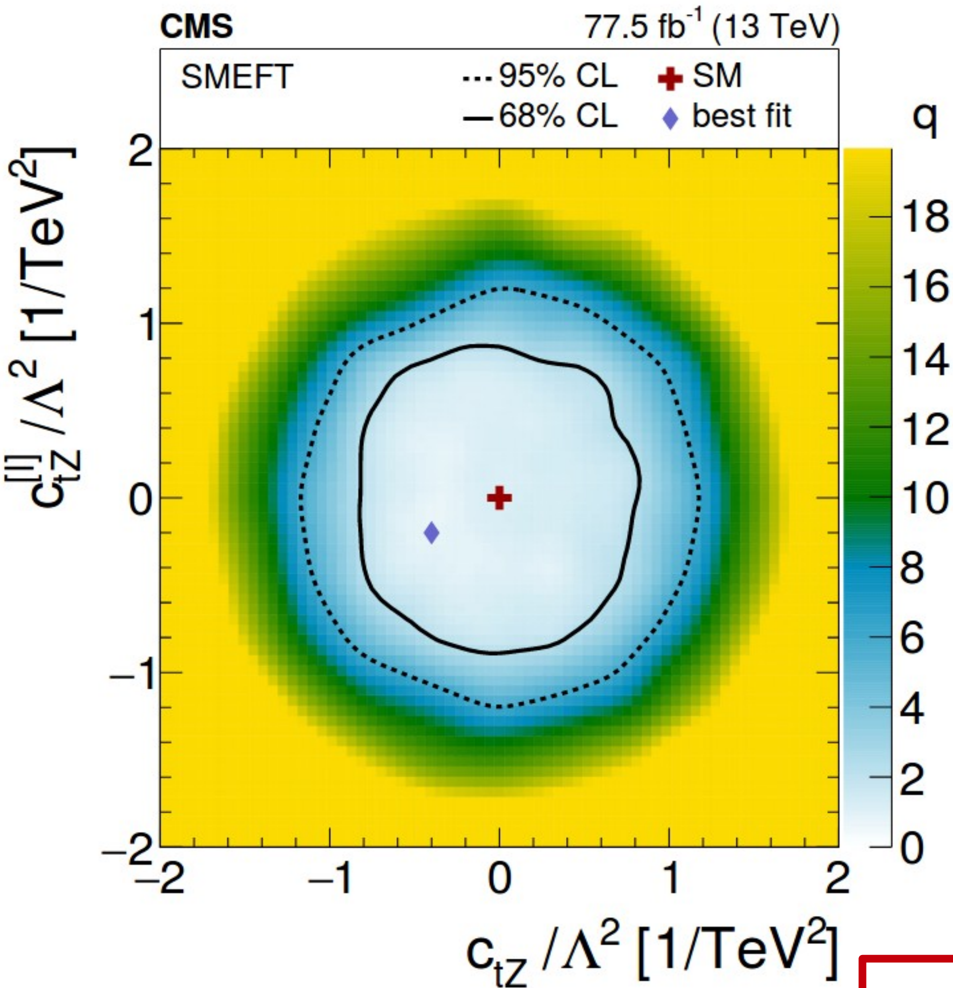

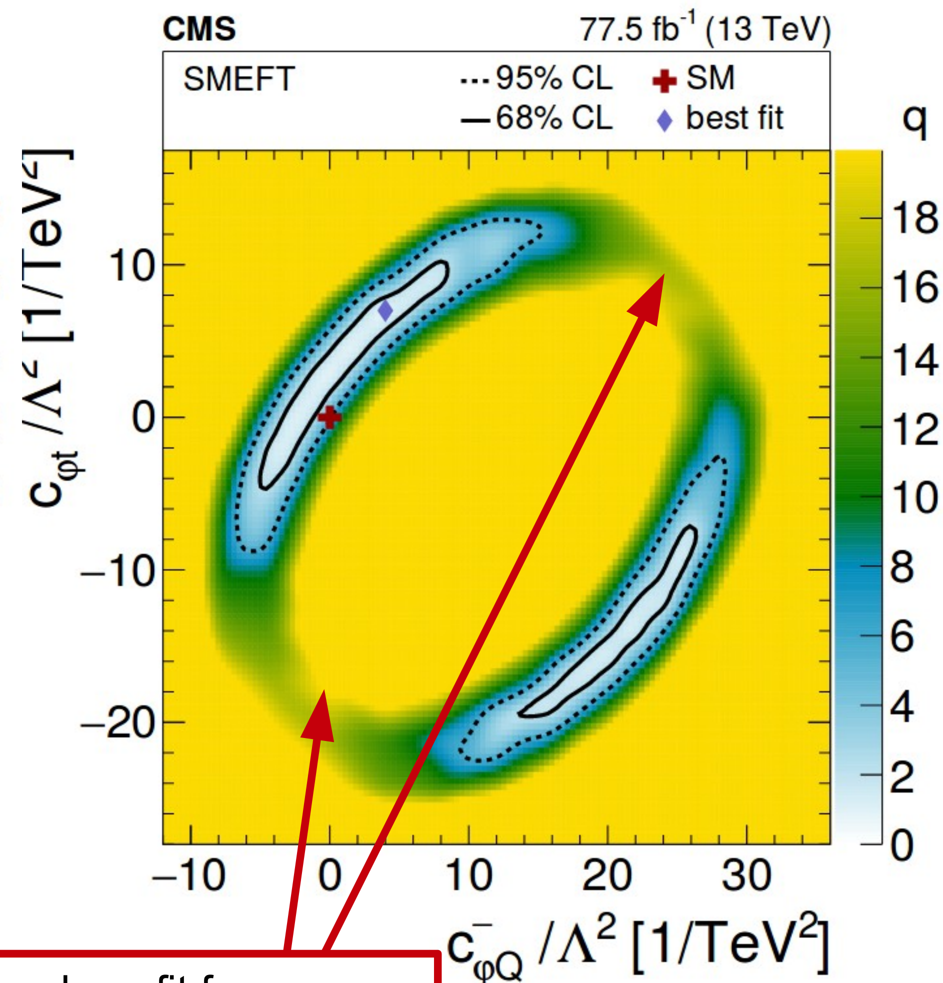

benefit from $p_T^Z/\cos(\Phi_Z^*)$ information

arXiv:1907.11270

Limits on anomalous top-Z couplings

- most stringent direct constraints on electroweak dipole moments and top-Z vector couplings (individual limits)
- PRD 99 (2019) 072009 :
  - limits from $t\bar{t}Z$ cross section in trilepton and tetralepton signal regions
  - NLO EFT cross section predictions
  - detector reconstruction efficiency verified to be compatible for SM and EFT

ATLAS

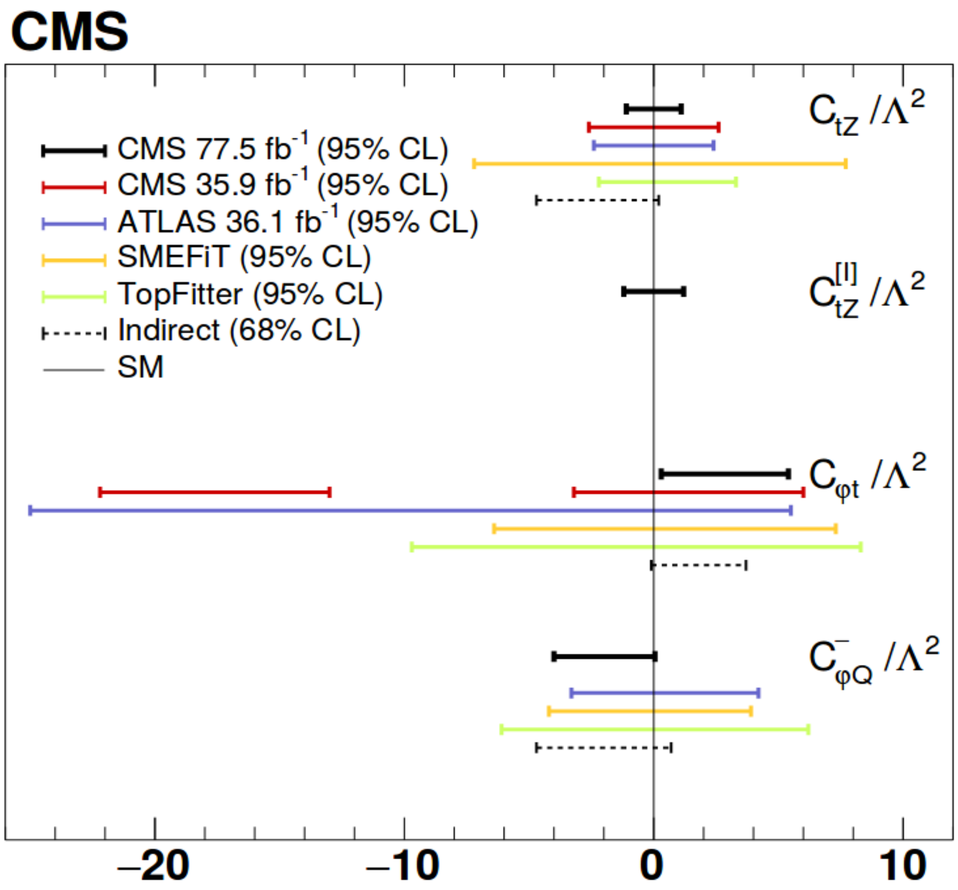

arXiv 1907.11270

EFT Approaches in ATLAS and CMS

hybrid measurement at detector-level

- (SM+EFT)/SM reweighting at generator-level, direct comparison to data
- take SM shape, estimate SM+EFT yields from simulation at generator

inclusive cross sections

- simple EFT parameterization sufficient

re-interpretation of unfolded measurement → direct measurement from detector-level data

unfolded, differential cross sections

- parton or particle level
- needs differential MC EFT information

direct measurement of EFT

- no SM assumption
- consider EFT in all relevant processes
- perform simultaneous fit to multiple regions

Probing simultaneously $t\bar{t}$ and tW production

- constraint separately 6 EFT couplings in dilepton final states

single top tW | $t\bar{t}$ | $t\bar{t}$ + single top tW

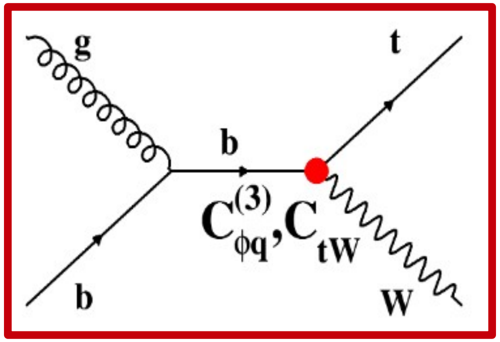

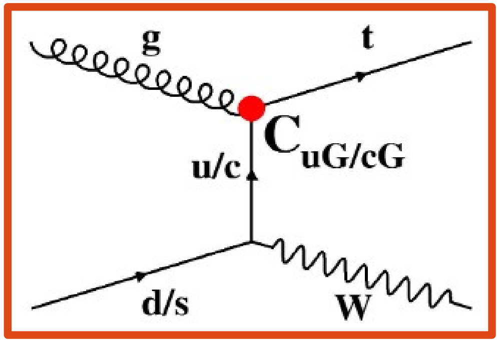

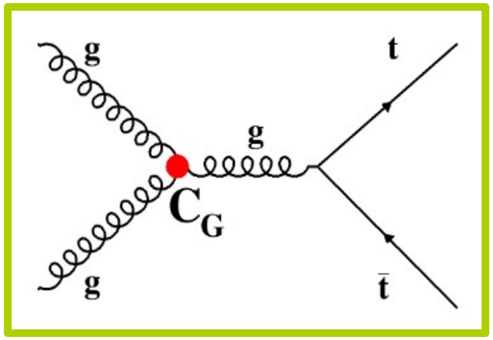

$$O_{tW} = (\bar{q}\sigma^{\mu\nu}\tau^i t)\tilde{\phi}W^i_{\mu\nu}$$

$$O^{(3)}_{\phi q} = (\phi^+\tau^i D_\mu \phi)(\bar{q}\gamma^\mu \tau^i q)$$

$$O_{u(c)G} = (\bar{q}\sigma^{\mu\nu}\lambda^a t)\tilde{\phi}G^a_{\mu\nu}.$$

$$O_G = f_{abc}G^{a\nu}_\mu G^{b\rho}_\nu G^{c\mu}_\rho.$$

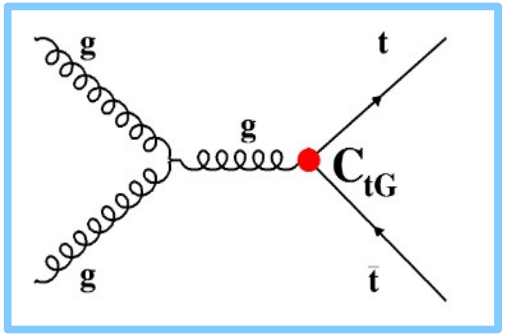

$$O_{tG} = (\bar{q}\sigma^{\mu\nu}\lambda^a t)\tilde{\phi}G^a_{\mu\nu}$$

Analysis strategy

- different categories of jet and b-jet multiplicities

Eff. coupling	Channel	Categories 1-jet ,0-tag	1-jet ,1-tag	2-jets,1-tag	>2-jets ,1-tag	≥2-jets,2-tags
	ee	—	Yield	Yield	—	Yield
C_G	$e\mu$	Yield	Yield	Yield	—	Yield
	$\mu\mu$	—	Yield	Yield	—	Yield
	ee	—	NN_{11}	NN_{21}	—	Yield
$C^{(3)}_{\phi q}$, C_{tW}, C_{tG}	$e\mu$	NN_{10}	NN_{11}	NN_{21}	—	Yield
	$\mu\mu$	—	NN_{11}	NN_{21}	—	Yield
	ee	—		NN_{FCNC}		—
C_{uG}, C_{cG}	$e\mu$	—		NN_{FCNC}		—
	$\mu\mu$	—		NN_{FCNC}		—

- dedicated NNs
  - to distinguish tW from $t\bar{t}$ topologies
  - to split FCNC from SM backgrounds

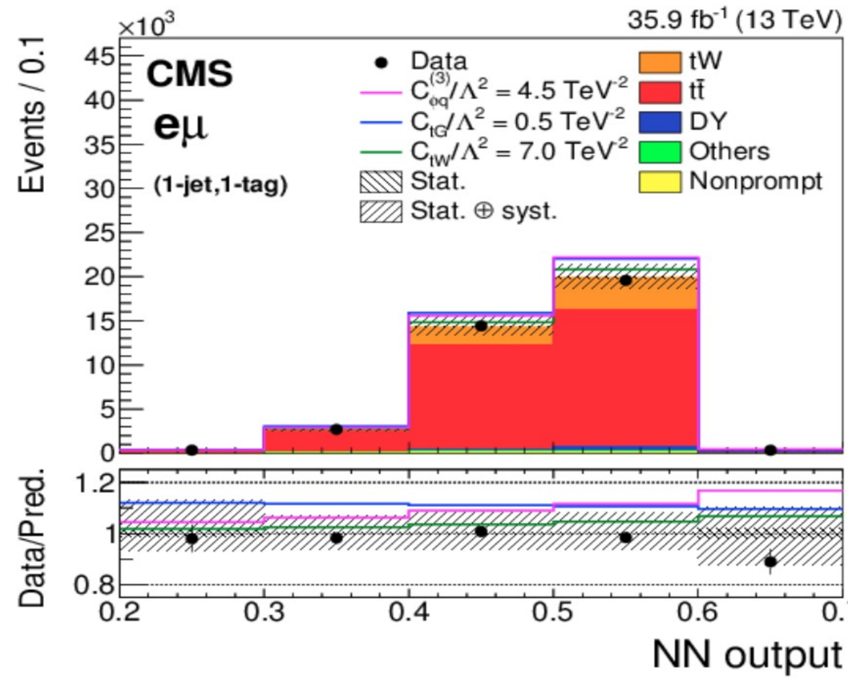

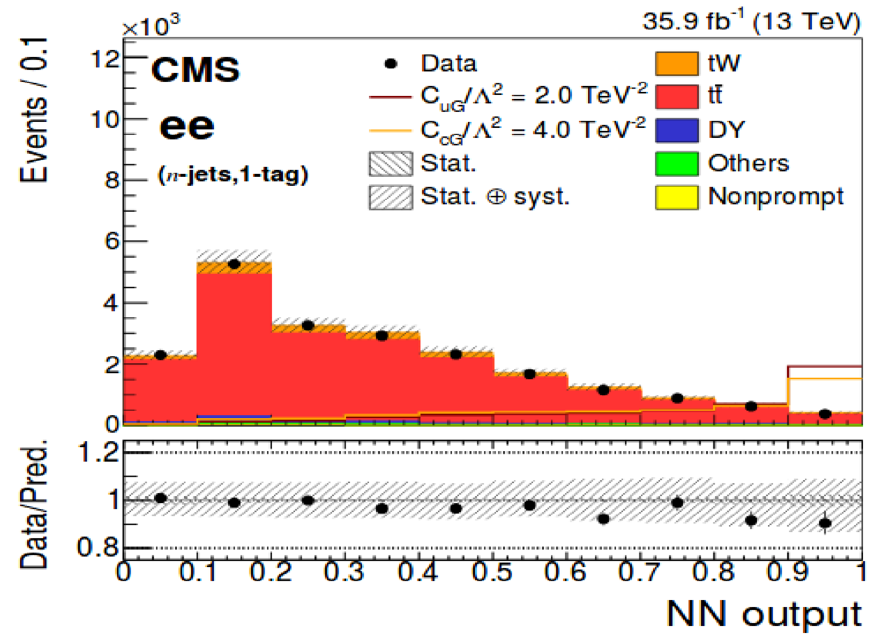

- limits on one operator at a time
  - all EFT cross sections at NLO in QCD (except for C_G)
  - dedicated LO simulation for tug/tcg
- sensitivity not at the level of more dedicated approaches, e.g. $-0.10 < C_{tG}/\Lambda^2 < 0.22$ TeV^{-2} in PRD 100,072002

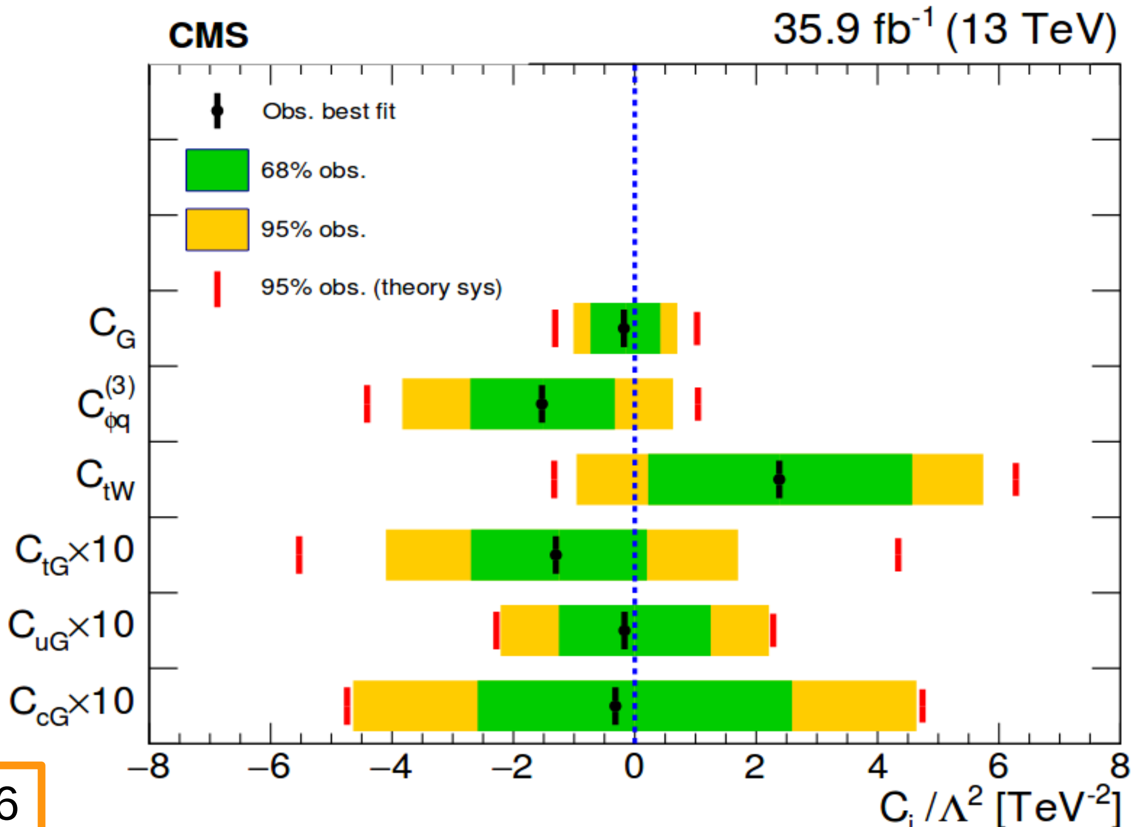

BR(t→ug)<0.12%

BR(t→cg) < 0.53 %

EPJ C 79 (2019) 886

EFT Approaches in ATLAS and CMS

inclusive cross sections

- simple EFT parameterization sufficient

hybrid measurement at detector-level

- (SM+EFT)/SM reweighting at generator-level, direct comparison to data
- take SM shape, estimate SM+EFT yields from simulation at generator

re-interpretation of unfolded measurement → direct measurement from detector-level data

unfolded, differential cross sections

- parton or particle level
- needs differential MC EFT information

direct measurement of EFT

- no SM assumption
- consider EFT in all relevant processes
- perform simultaneous fit to multiple regions

Photon FCNC analysis strategy

- explore both production (single top) and decay (tt̄)
  - single top particularly interesting as left-handed (LH) and right-handed (RH) couplings differently impact kinematics of top decay products

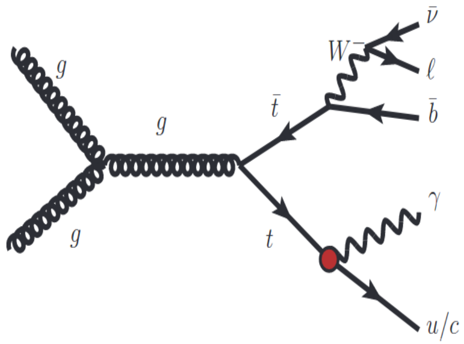

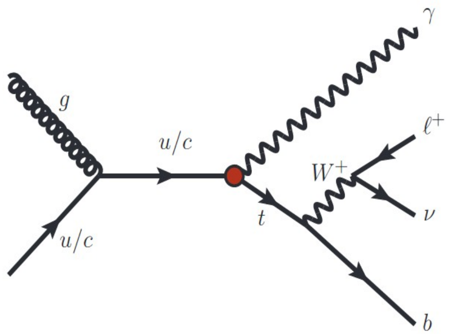

SR definition enhancing production

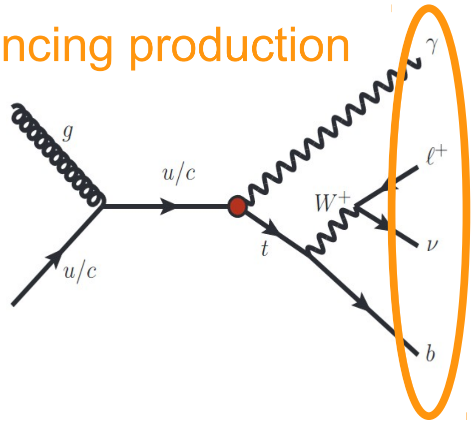

- explore both production (single top) and decay $(t\bar{t})$
  - single top particularly interesting as left-handed (LH) and right-handed (RH) couplings differently impact kinematics of top decay products

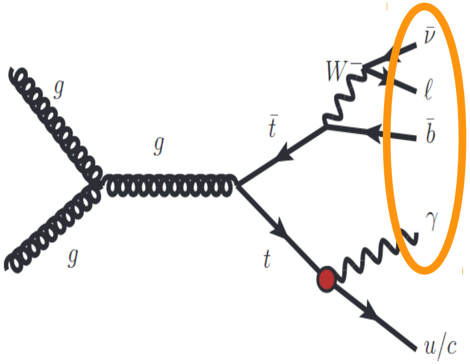

Photon FCNC analysis strategy

SR definition enhancing production

- explore both production (single top) and decay ($t\bar{t}$)
  - single top particularly interesting as left-handed (LH) and right-handed (RH) couplings differently impact kinematics of top decay products

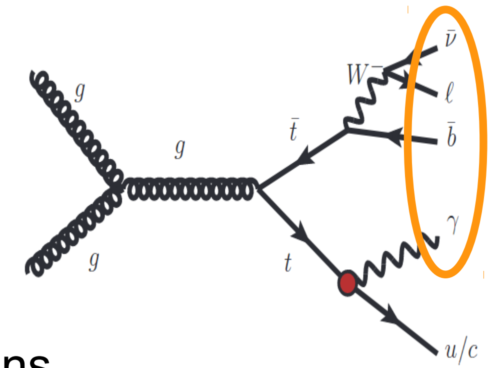

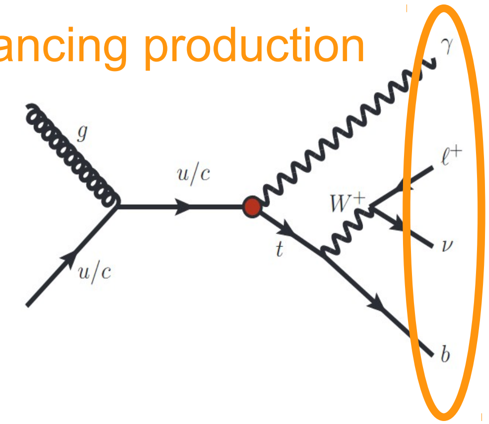

- main background: $t\bar{t}$ with misidentified electrons
  - scaling of fake photon events from data
- dedicated CR's for W/Z + γ + jets

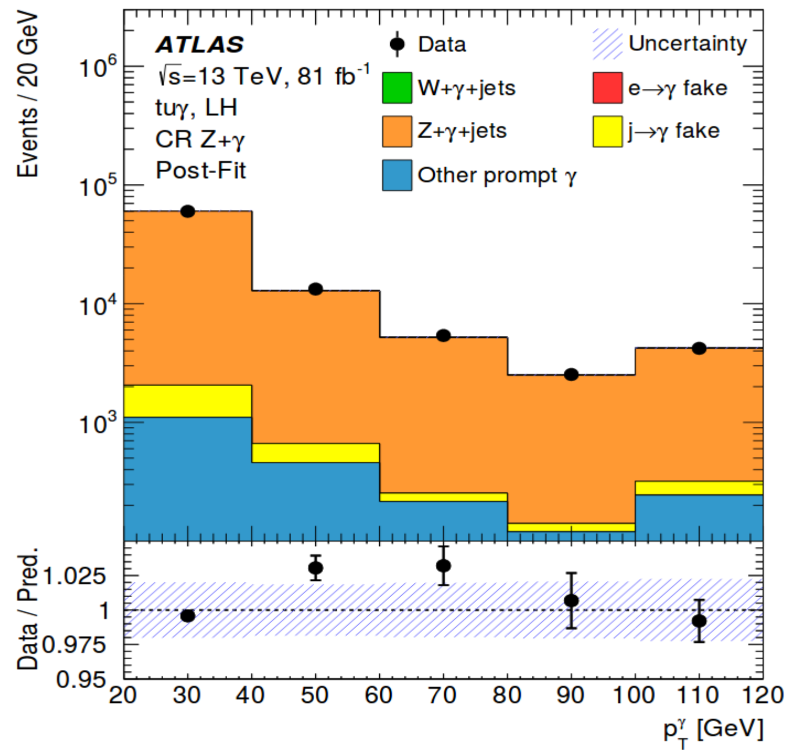

Photon FCNC analysis strategy

- explore both production (single top) and decay ($t\bar{t}$)
  - single top particularly interesting as left-handed (LH) and right-handed (RH) couplings differently impact kinematics of top decay products

SR definition enhancing production

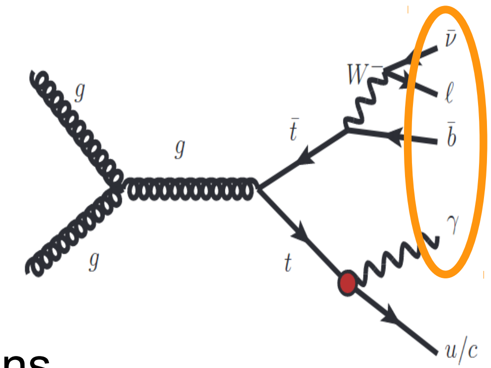

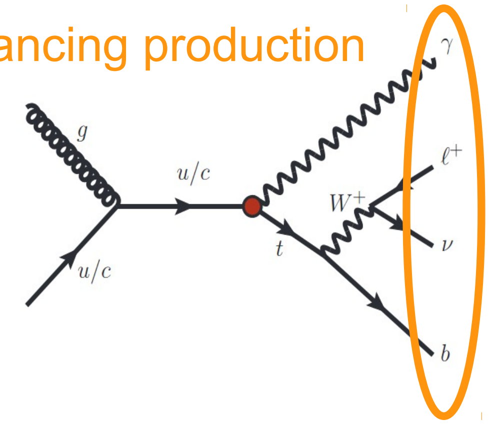

- main background: $t\bar{t}$ with misidentified electrons
  - scaling of fake photon events from data
- dedicated CR's for W/Z + γ + jets
- MVA to probe tiny signal
  - separate NNs for tuγ/tcγ and LH/RH
  - use basic properties like p_T, invariant masses and distances

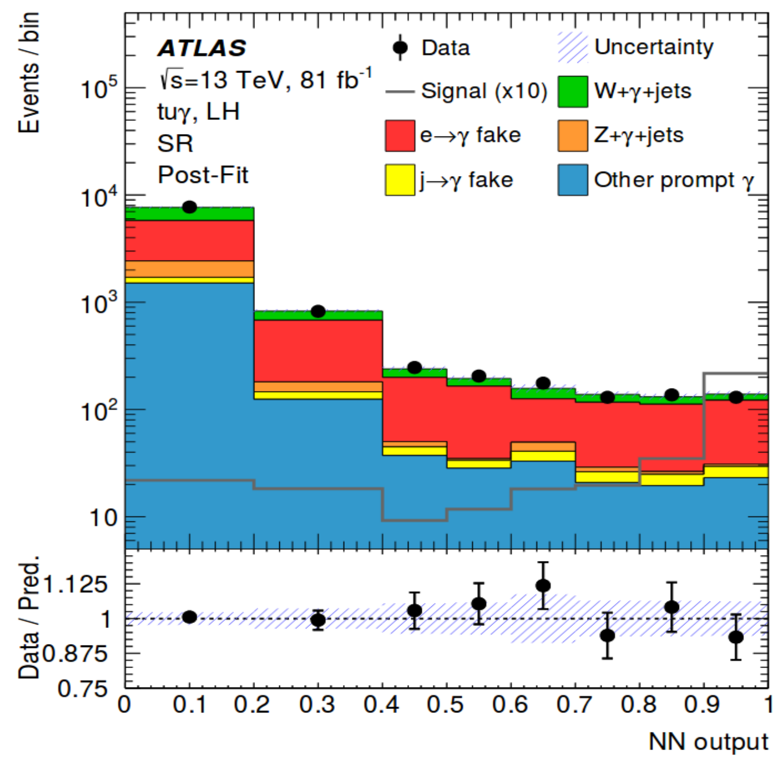

Photon FCNC constrains on EFT

- constraint EFT operators based on NLO TopFCNC model

FCNC tensor couplings :

$$O_{uB}^{(ij)} = (\bar{q}_i \sigma^{\mu\nu} u_j) \quad \tilde{\varphi} B_{\mu\nu}$$

$$O_{uW}^{(ij)} = (\bar{q}_i \sigma^{\mu\nu} \tau^I u_j) \, \tilde{\varphi} W_{\mu\nu}^I$$

LH limits slightly more stringent because of different decay kinematics

Observable	Vertex	Coupling	Obs.	Exp.
$\lvert C_{uW}^{(13)*} + C_{uB}^{(13)*} \rvert$	$tu\gamma$	LH	0.19	$0.22^{+0.04}_{-0.03}$
$\lvert C_{uW}^{(31)} + C_{uB}^{(31)} \rvert$	$tu\gamma$	RH	0.27	$0.27^{+0.05}_{-0.04}$
$\lvert C_{uW}^{(23)*} + C_{uB}^{(23)*} \rvert$	$tc\gamma$	LH	0.52	$0.57^{+0.11}_{-0.09}$
$\lvert C_{uW}^{(32)} + C_{uB}^{(32)} \rvert$	$tc\gamma$	RH	0.48	$0.59^{+0.12}_{-0.09}$

SR definition enhances contribution from FCNC production over decay: 4 time more production/decay for up, less than the same for charm

- largest systematics from jet energy resolution and modeling (e.g photon pT reweighting, ME scale)

PLB 800 (2019) 135082

Summary

- precision SMEFT measurements will be an essential part of the LHC heritage
- the LHC has entered an EFT era
  - large variety of 13 TeV results already available
- first strategies for more global LHC SMEFT measurements established
- need to combine efforts across existing research groups
- right time to re-think and improve research strategies
- still many unexplored processes

Back-Up

SMEFT in a Nutshell

- SM effective field theory (SMEFT)

$$L = L_{SM}^{(4)} + \sum_i \frac{c_i^{(5)}}{\Lambda_i} O_i^{(5)} + \sum_i \frac{c_i^{(6)}}{\Lambda_i^2} O_i^{(6)} + \ldots$$

- operator expansion:
  - heavy BSM states are integrated out
  - only local operators from SM fields left
- truncated at dimension 6 (leading B & L preserving interactions)
- order-by-order: self-consistent, renormalizable QFT
- can be matched to UV theories of new physics

Dimension-6 SMEFT Operators

X^3		φ^6 and $\varphi^4 D^2$		$\psi^2\varphi^3$	
Q_G	$f^{ABC} G_\mu^{A\nu} G_\nu^{B\rho} G_\rho^{C\mu}$	Q_φ	$(\varphi^\dagger\varphi)^3$	$Q_{e\varphi}$	$(\varphi^\dagger\varphi)(\bar l_p e_r \varphi)$
$Q_{\widetilde G}$	$f^{ABC} \widetilde G_\mu^{A\nu} G_\nu^{B\rho} G_\rho^{C\mu}$	$Q_{\varphi\Box}$	$(\varphi^\dagger\varphi)\Box(\varphi^\dagger\varphi)$	$Q_{u\varphi}$	$(\varphi^\dagger\varphi)(\bar q_p u_r \widetilde\varphi)$
Q_W	$\varepsilon^{IJK} W_\mu^{I\nu} W_\nu^{J\rho} W_\rho^{K\mu}$	$Q_{\varphi D}$	$\left(\varphi^\dagger D^\mu\varphi\right)^\star \left(\varphi^\dagger D_\mu\varphi\right)$	$Q_{d\varphi}$	$(\varphi^\dagger\varphi)(\bar q_p d_r \varphi)$
$Q_{\widetilde W}$	$\varepsilon^{IJK} \widetilde W_\mu^{I\nu} W_\nu^{J\rho} W_\rho^{K\mu}$				
$X^2\varphi^2$		$\psi^2 X\varphi$		$\psi^2\varphi^2 D$	
$Q_{\varphi G}$	$\varphi^\dagger\varphi\, G^A_{\mu\nu} G^{A\mu\nu}$	Q_{eW}	$(\bar l_p \sigma^{\mu\nu} e_r) \tau^I \varphi W_{\mu\nu}^I$	$Q_{\varphi l}^{(1)}$	$(\varphi^\dagger i\overleftrightarrow{D}_\mu \varphi)(\bar l_p \gamma^\mu l_r)$
$Q_{\varphi\widetilde G}$	$\varphi^\dagger\varphi\, \widetilde G^A_{\mu\nu} G^{A\mu\nu}$	Q_{eB}	$(\bar l_p \sigma^{\mu\nu} e_r) \varphi B_{\mu\nu}$	$Q_{\varphi l}^{(3)}$	$(\varphi^\dagger i\overleftrightarrow{D}^I_\mu \varphi)(\bar l_p \tau^I \gamma^\mu l_r)$
$Q_{\varphi W}$	$\varphi^\dagger\varphi\, W^I_{\mu\nu} W^{I\mu\nu}$	Q_{uG}	$(\bar q_p \sigma^{\mu\nu} T^A u_r) \widetilde\varphi\, G_{\mu\nu}^A$	$Q_{\varphi e}$	$(\varphi^\dagger i\overleftrightarrow{D}_\mu \varphi)(\bar e_p \gamma^\mu e_r)$
$Q_{\varphi\widetilde W}$	$\varphi^\dagger\varphi\, \widetilde W^I_{\mu\nu} W^{I\mu\nu}$	Q_{uW}	$(\bar q_p \sigma^{\mu\nu} u_r) \tau^I \widetilde\varphi\, W_{\mu\nu}^I$	$Q_{\varphi q}^{(1)}$	$(\varphi^\dagger i\overleftrightarrow{D}_\mu \varphi)(\bar q_p \gamma^\mu q_r)$
$Q_{\varphi B}$	$\varphi^\dagger\varphi\, B_{\mu\nu} B^{\mu\nu}$	Q_{uB}	$(\bar q_p \sigma^{\mu\nu} u_r) \widetilde\varphi\, B_{\mu\nu}$	$Q_{\varphi q}^{(3)}$	$(\varphi^\dagger i\overleftrightarrow{D}^I_\mu \varphi)(\bar q_p \tau^I \gamma^\mu q_r)$
$Q_{\varphi\widetilde B}$	$\varphi^\dagger\varphi\, \widetilde B_{\mu\nu} B^{\mu\nu}$	Q_{dG}	$(\bar q_p \sigma^{\mu\nu} T^A d_r) \varphi\, G_{\mu\nu}^A$	$Q_{\varphi u}$	$(\varphi^\dagger i\overleftrightarrow{D}_\mu \varphi)(\bar u_p \gamma^\mu u_r)$
$Q_{\varphi WB}$	$\varphi^\dagger\tau^I\varphi\, W^I_{\mu\nu} B^{\mu\nu}$	Q_{dW}	$(\bar q_p \sigma^{\mu\nu} d_r) \tau^I \varphi\, W_{\mu\nu}^I$	$Q_{\varphi d}$	$(\varphi^\dagger i\overleftrightarrow{D}_\mu \varphi)(\bar d_p \gamma^\mu d_r)$
$Q_{\varphi\widetilde WB}$	$\varphi^\dagger\tau^I\varphi\, \widetilde W^I_{\mu\nu} B^{\mu\nu}$	Q_{dB}	$(\bar q_p \sigma^{\mu\nu} d_r) \varphi\, B_{\mu\nu}$	$Q_{\varphi ud}$	$i(\widetilde\varphi^\dagger D_\mu \varphi)(\bar u_p \gamma^\mu d_r)$

Table 2: Dimension-six operators other than the four-fermion ones.

$(\bar LL)(\bar LL)$		$(\bar RR)(\bar RR)$		$(\bar LL)(\bar RR)$	
Q_{ll}	$(\bar l_p \gamma_\mu l_r)(\bar l_s \gamma^\mu l_t)$	Q_{ee}	$(\bar e_p \gamma_\mu e_r)(\bar e_s \gamma^\mu e_t)$	Q_{le}	$(\bar l_p \gamma_\mu l_r)(\bar e_s \gamma^\mu e_t)$
$Q_{qq}^{(1)}$	$(\bar q_p \gamma_\mu q_r)(\bar q_s \gamma^\mu q_t)$	Q_{uu}	$(\bar u_p \gamma_\mu u_r)(\bar u_s \gamma^\mu u_t)$	Q_{lu}	$(\bar l_p \gamma_\mu l_r)(\bar u_s \gamma^\mu u_t)$
$Q_{qq}^{(3)}$	$(\bar q_p \gamma_\mu \tau^I q_r)(\bar q_s \gamma^\mu \tau^I q_t)$	Q_{dd}	$(\bar d_p \gamma_\mu d_r)(\bar d_s \gamma^\mu d_t)$	Q_{ld}	$(\bar l_p \gamma_\mu l_r)(\bar d_s \gamma^\mu d_t)$
$Q_{lq}^{(1)}$	$(\bar l_p \gamma_\mu l_r)(\bar q_s \gamma^\mu q_t)$	Q_{eu}	$(\bar e_p \gamma_\mu e_r)(\bar u_s \gamma^\mu u_t)$	Q_{qe}	$(\bar q_p \gamma_\mu q_r)(\bar e_s \gamma^\mu e_t)$
$Q_{lq}^{(3)}$	$(\bar l_p \gamma_\mu \tau^I l_r)(\bar q_s \gamma^\mu \tau^I q_t)$	Q_{ed}	$(\bar e_p \gamma_\mu e_r)(\bar d_s \gamma^\mu d_t)$	$Q_{qu}^{(1)}$	$(\bar q_p \gamma_\mu q_r)(\bar u_s \gamma^\mu u_t)$
		$Q_{ud}^{(1)}$	$(\bar u_p \gamma_\mu u_r)(\bar d_s \gamma^\mu d_t)$	$Q_{qu}^{(8)}$	$(\bar q_p \gamma_\mu T^A q_r)(\bar u_s \gamma^\mu T^A u_t)$
		$Q_{ud}^{(8)}$	$(\bar u_p \gamma_\mu T^A u_r)(\bar d_s \gamma^\mu T^A d_t)$	$Q_{qd}^{(1)}$	$(\bar q_p \gamma_\mu q_r)(\bar d_s \gamma^\mu d_t)$
				$Q_{qd}^{(8)}$	$(\bar q_p \gamma_\mu T^A q_r)(\bar d_s \gamma^\mu T^A d_t)$
$(\bar LR)(\bar RL)$ and $(\bar LR)(\bar LR)$		B-violating			
Q_{ledq}	$(\bar l_p^j e_r)(\bar d_s q_t^j)$	Q_{duq}	$\varepsilon^{\alpha\beta\gamma}\varepsilon_{jk}\left[(d_p^\alpha)^T C u_r^\beta\right]\left[(q_s^{\gamma j})^T C l_t^k\right]$		
$Q_{quqd}^{(1)}$	$(\bar q_p^j u_r)\varepsilon_{jk}(\bar q_s^k d_t)$	Q_{qqu}	$\varepsilon^{\alpha\beta\gamma}\varepsilon_{jk}\left[(q_p^{\alpha j})^T C q_r^{\beta k}\right]\left[(u_s^\gamma)^T C e_t\right]$		
$Q_{quqd}^{(8)}$	$(\bar q_p^j T^A u_r)\varepsilon_{jk}(\bar q_s^k T^A d_t)$	Q_{qqq}	$\varepsilon^{\alpha\beta\gamma}\varepsilon_{jn}\varepsilon_{km}\left[(q_p^{\alpha j})^T C q_r^{\beta k}\right]\left[(q_s^{\gamma m})^T C l_t^n\right]$		
$Q_{lequ}^{(1)}$	$(\bar l_p^j e_r)\varepsilon_{jk}(\bar q_s^k u_t)$	Q_{duu}	$\varepsilon^{\alpha\beta\gamma}\left[(d_p^\alpha)^T C u_r^\beta\right]\left[(u_s^\gamma)^T C e_t\right]$		
$Q_{lequ}^{(3)}$	$(\bar l_p^j \sigma_{\mu\nu} e_r)\varepsilon_{jk}(\bar q_s^k \sigma^{\mu\nu} u_t)$				

Table 3: Four-fermion operators.

- complete, non-redundant set of operators:
  - dimension-6: 59 (76 real)
  - depending on CP/flavor assumptions

Probing top-W couplings with single top quarks

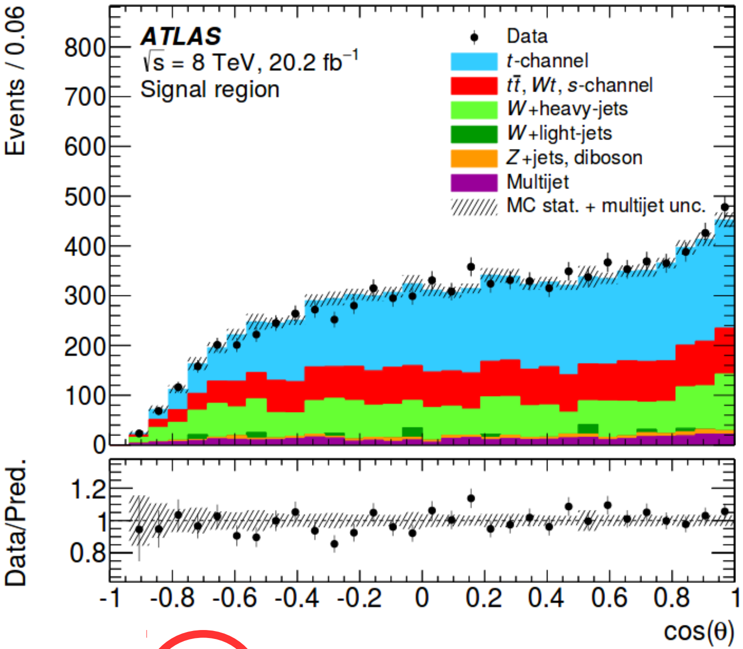

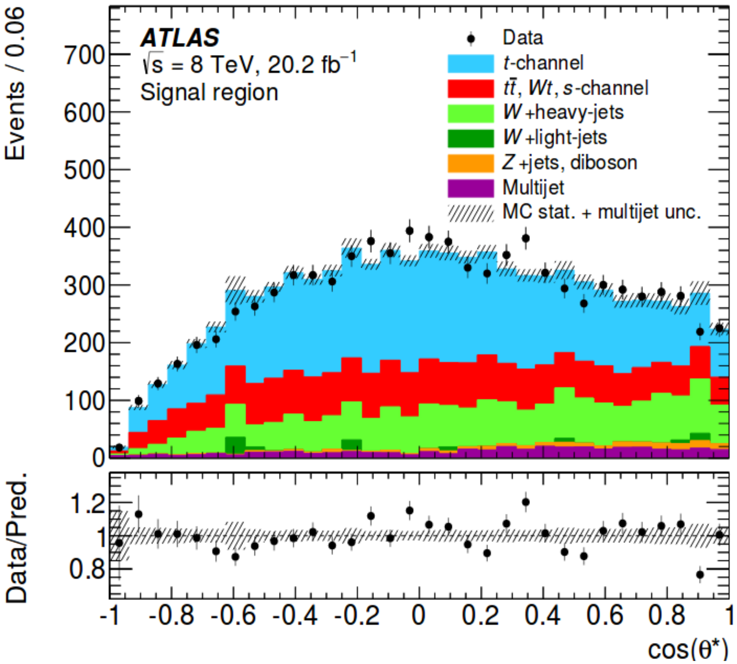

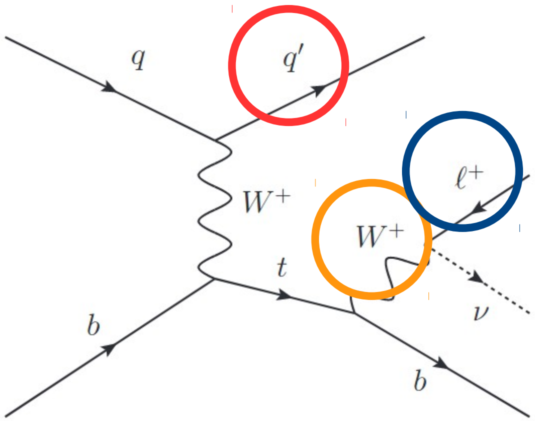

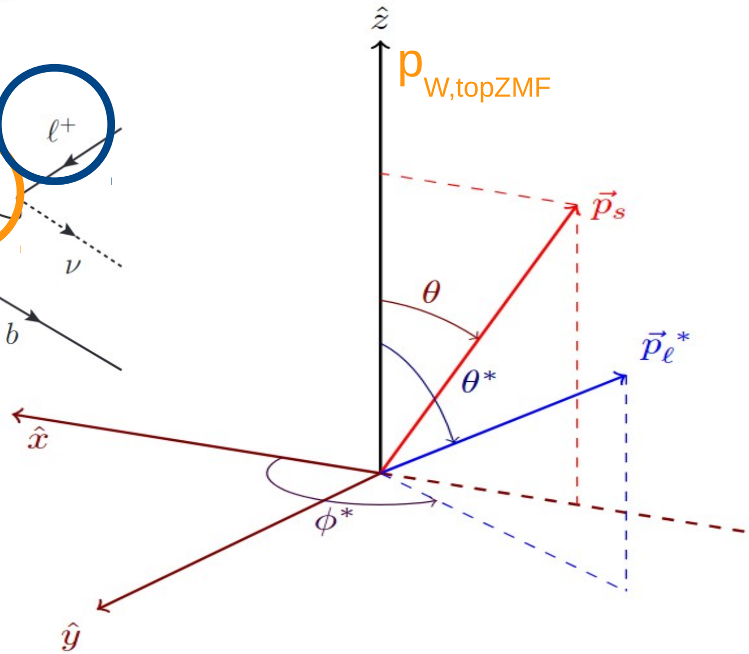

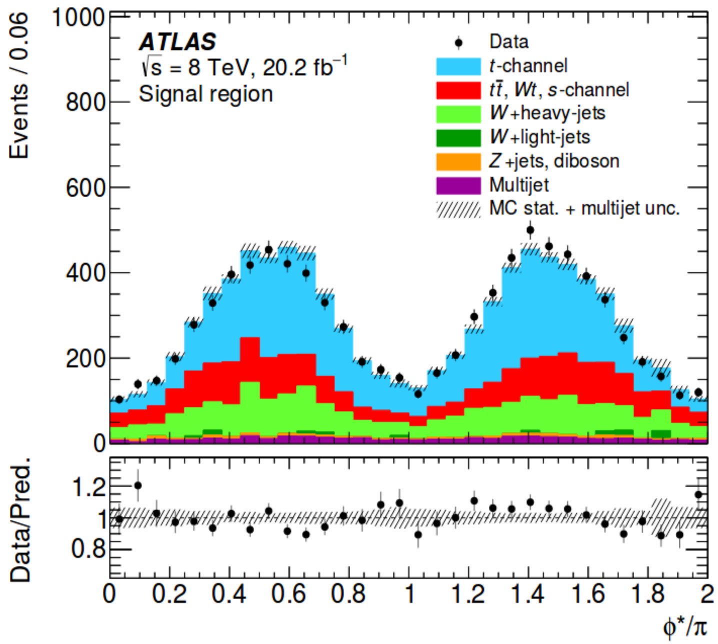

ttZ 2016 + 2017

- improved analysis strategy:
  - more inclusive trigger
  - multivariate lepton identification (x2 syst. red.)
  - better lepton and efficiency measurements
  - (~15% higher prompt-lepton efficiency)

Source	Uncertainty range (%)	Correlated in 2016 and 2017	Impact on the $t\bar{t}Z$ cross section (%)
Integrated luminosity	2.5	×	2
PU modeling	1–2	✓	1
Trigger	2	×	2
Lepton ID efficiency	4.5–6	✓	4
Jet energy scale	1–9	✓	2
Jet energy resolution	0–1	✓	1
B tagging light flavor	0–4	×	1
B tagging heavy flavor	1–4	×	2
Choice in μ_R and μ_F	1–4	✓	1
PDF choice	1–2	✓	1
Color reconnection	1.5	✓	<1
Parton shower	1–8	✓	1
WZ cross section	10–20	✓	3
WZ + heavy flavor	8	✓	1
ZZ cross section	10	✓	1
$t(\bar{t})X$ bg.	10–15	✓	3
$X\gamma$ background	20	✓	1
Nonprompt background	30	✓	<1
Rare SM background	50	✓	2
Stat. unc. in nonprompt bg.	5–50	×	<1
Stat. unc. in rare SM bg.	5–100	×	<1
Total uncertainty			7

$t\bar{t}Z$ results from ATLAS

Coefficients	$C_{\phi Q}^{(3)}/\Lambda^2$	$C_{\phi t}/\Lambda^2$	C_{tB}/Λ^2	C_{tW}/Λ^2
Previous indirect constraints at 68% CL	[–4.7, 0.7]	[–0.1, 3.7]	[–0.5, 10]	[–1.6, 0.8]
Previous direct constraints at 95% CL	[–1.3, 1.3]	[–9.7, 8.3]	[–6.9, 4.6]	[–0.2, 0.7]
Expected limit at 68% CL	[–2.1, 1.9]	[–3.8, 2.7]	[–2.9, 3.0]	[–1.8, 1.9]
Expected limit at 95% CL	[–4.5, 3.6]	[–23, 4.9]	[–4.2, 4.3]	[–2.6, 2.6]
Observed limit at 68% CL	[–1.0, 2.7]	[–2.0, 3.5]	[–3.7, 3.5]	[–2.2, 2.1]
Observed limit at 95% CL	[–3.3, 4.2]	[–25, 5.5]	[–5.0, 5.0]	[–2.9, 2.9]
Expected limit at 68% CL (linear)	[–1.9, 2.0]	[–3.0, 3.2]	–	–
Expected limit at 95% CL (linear)	[–3.7, 4.0]	[–5.8, 6.3]	–	–
Observed limit at 68% CL (linear)	[–1.0, 2.9]	[–1.8, 4.4]	–	–
Observed limit at 95% CL (linear)	[–2.9, 4.9]	[–4.8, 7.5]	–	–

A global,experimental analysis of the top-quark sector

- individual measurements of top, Higgs and electroweak processes not easily lend themselves to EFT interpretation
  - e.g. “backgrounds” of $t\bar{t}Z$ cross sections like $t\bar{t}W$, $t\bar{t}H$, tqZ, tHq,… also affected by EFT
  - considerable statistical overlap between different measurements

- consistent treatment crucial
  - theory model
  - systematic uncertainties
  - correlations across measurements

- intrinsically small effects
  - precise theoretical control
  - excellent experimental precision

→ a global effort including the experimental and theoretical LHC communities desirable

Towards Global Analysis

- LHC Top working group:
  - common EFT model: dim6top (arXiv 1802.07237)
  - re-interpretation of unfolded results
    - good scalability, easy combinable beyond LHC
    - treat background SM-like
    - full phase space results sensitive to efficiency/acceptance differences
      → fiducial, particle level
  - measurements at detector level
    - good sensitivity
    - probe EFT in all contributing processes
    - so far relying on MC reweighing → further developments crucial
    - several options for later combinations

Probing Z FCNC in trilepton final states

- complementary probe of O_{uB} and O_{uW} from tZu/tZc FCNC

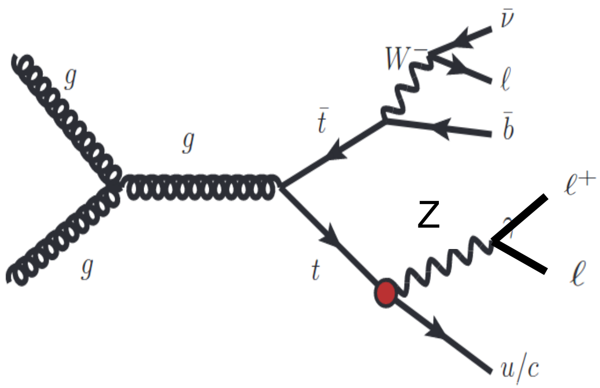

- focus on $t\bar{t}$ production

- perform event reconstruction to match

$$\chi^2 = \frac{\left(m^{\text{reco}}_{j_a\ell_a\ell_b} - m_{t_{\text{FCNC}}}\right)^2}{\sigma^2_{t_{\text{FCNC}}}} + \frac{\left(m^{\text{reco}}_{j_b\ell_c\nu} - m_{t_{\text{SM}}}\right)^2}{\sigma^2_{t_{\text{SM}}}} + \frac{\left(m^{\text{reco}}_{\ell_c\nu} - m_W\right)^2}{\sigma^2_W}$$

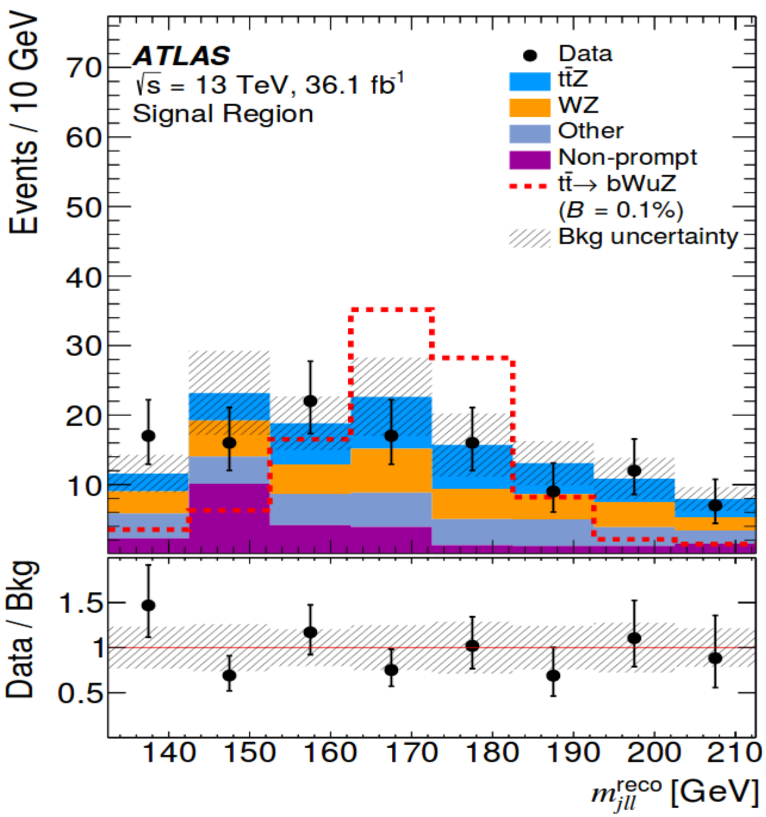

Z FCNC constrains on EFT

- simultaneous fit to SR and 5 CRs to constraint backgrounds and reduce systematics

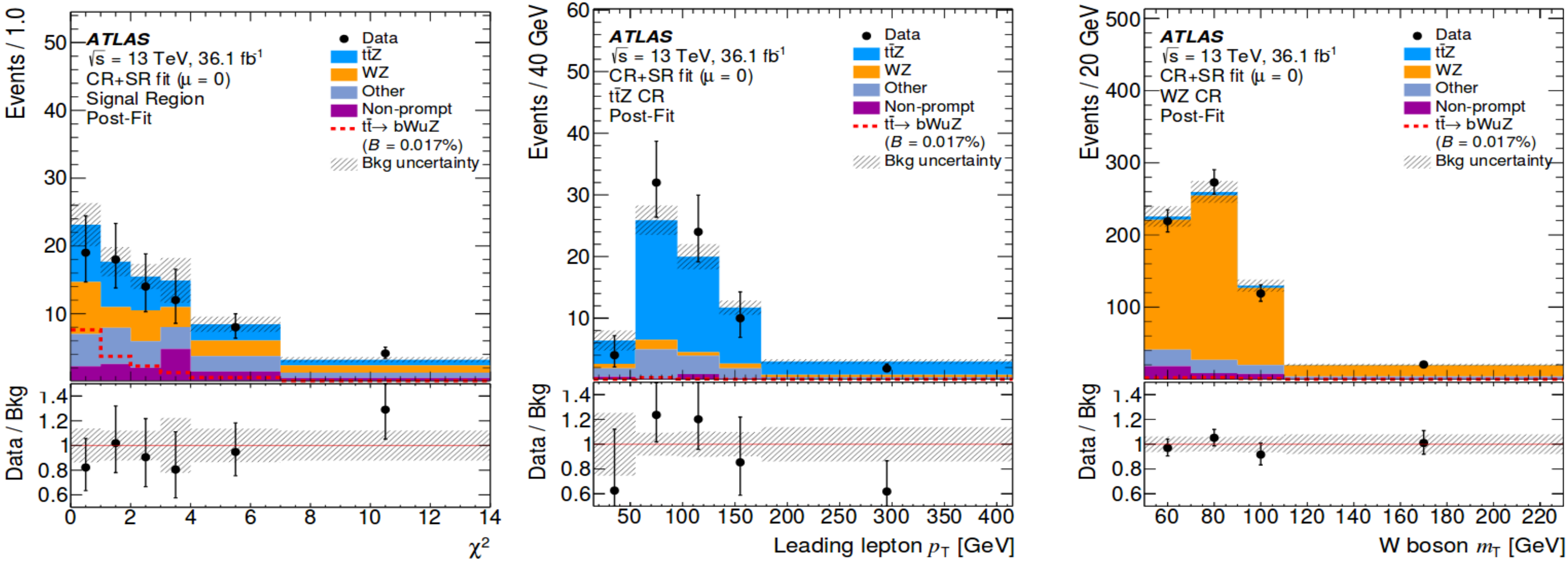

- constraint EFT based on NLO TopFCNC model
  - only one operator non-zero at a time
- largest systematics from event modeling

Operator	Observed	Expected
$\lvert C_{uB}^{(31)} \rvert$	0.25	0.30
$\lvert C_{uW}^{(31)} \rvert$	0.25	0.30
$\lvert C_{uB}^{(32)} \rvert$	0.30	0.34
$\lvert C_{uW}^{(32)} \rvert$	0.30	0.34

PLB 800 (2019) 135082

Flavor changing neutral currents

- forbidden at tree level and suppressed by GIM mechanism by ~14 orders of magnitude

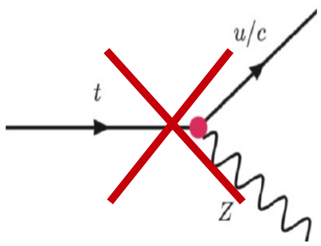

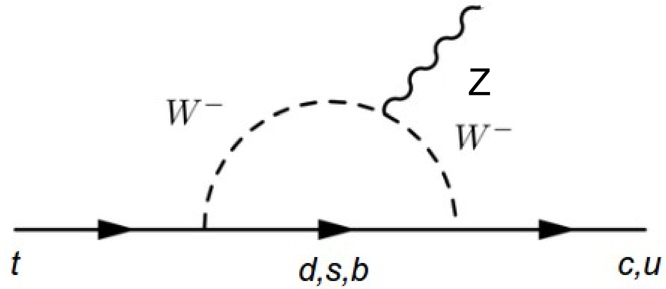

- large variety of LHC analyses searching for FCNC through Higgs/Z/photon/gluon
  - single top production and t$\bar{t}$ decay